

AAAS Conference: “2nd Law Challenges” University of San Diego 2016

Maxwell Demons by Phase Transitions Severing the link between Physics and Information Theory

Remi Cornwall

University of London Alumni Society, Malet Street, London WC1E 7HU

<http://webspaces.qmul.ac.uk/roccornwall> http://www.researchgate.net/profile/Remi_Cornwall

Abstract

The search for new power sources has increasingly challenged the second law of thermodynamics; one such cycle is presented herein with both experimental and rigorous theoretical underpinnings. These analyses, both kinetic and thermodynamic inevitably lead to the Maxwell Demon problem. It is clear that, against the Szilard-Brillouin-Landauer argument, that phase transition processes in conjunction with the cycle and apparatus requires no molecular information to be kept, negating the argument and need that the demon’s entropy change by $1/2kT \ln 2$ per molecule processed. The Demon was thought to bring Information into the fold of Physics. We ask the question, if all computing can be made reversible by heat recovery and furthermore, if the speed of information appears not to be limited by Relativity, due to the author’s protocol to send classical data over an entangled Bell Channel, if the Landauer maxim, “Information is Physical”, is entirely true?

1. Introduction

Thermodynamics is eclectic covering “prosaic concerns” of steam engines and power generation for a burgeoning 21st century civilisation, Life, Cosmology and even Information Theory. It is inevitable, just as its inception, that practical concerns have the deepest impact in theoretical physics. Given the spate of publications challenging the second law[1-4], we present a new thermodynamic cycle which bears similarity to conventional magneto-calorific effect devices but extends the theory beyond these realms, whilst keeping a footing firmly in experimental actuality by utilising thermodynamics, kinetic theory and the magneto-dynamics of ferrofluids.

The next section finds the underlying reason of why such processes are permitted and links trajectories on a T-S diagram (or P-V diagram), in conventional thermodynamic reasoning regarding cyclical processes, to the working substance undergoing phase change, to a molecular sorting process viewed from the kinetic theory perspective. This clearly invokes Maxwell’s Demon. The flaws in the anti-demon arguments are then recounted to note that natural kinetic processes require no computing equipment, memory storage or erasure of memory step; the sorting is inherent.

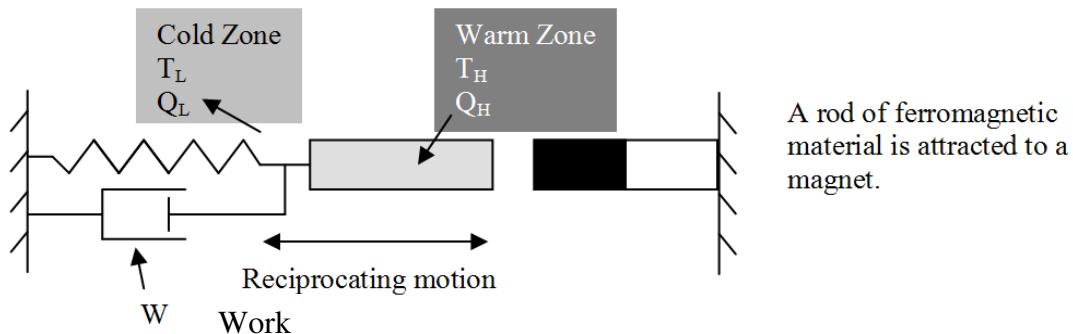
20 Finally the author briefly summarises their work in another field that asks the question,
21 “What is the ultimate speed of information”? The Demon problem was meant to bring
22 Information into the sphere of physical understanding by the link with thermodynamics, if
23 de-facto reversible computing is possible by heat recovery by the cycles discussed herein and
24 elsewhere *and furthermore*, the speed of information transit is not governed by Relativity,
25 how can Landauer’s claim that “Information is physical” be entirely true? Information
26 appears to take on *at least* a mathematical, if not *metaphysical* aspect.
27

28 **2. The Limitation of Magneto-calorific Effect Carnot** 29 **cycles**

30
31 We shall focus on magnetic heat engines to arrive at our second law challenging mechanism.
32 First, the state of the art in conventional magneto-calorific effect engines is discussed, to
33 reassure the reader about the commonplace phenomena and analysis and where the train of
34 thought can lead one, if not least to show that conventional thought is creaking at the seams.
35 The impetus for magnetic heat engine research is the potential of having machines with few
36 moving parts, high efficiency and low environmental impact.
37

38 Magnetic heat engines need a variation of magnetisation with temperature and two effects are
39 noted: the force experienced by magnetic materials in an external field[5-7] (\mathcal{M} is the volume
40 magnetisation) and the magneto-caloric effect[8-11].
41

$$F = -\nabla(\mathcal{M} \cdot \mathbf{B}) \quad \text{eqn. 1}$$



44
45
46
47
48 **Figure 1 – A Simple Reciprocating**
49 **Magnetic Motor**

50
51
52

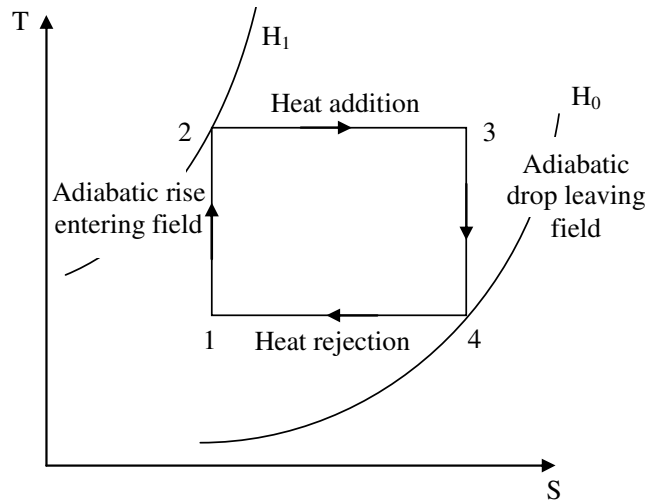


Figure 2 – T-S diagram, Magnetic Heat Engine

Figure 1 shows a means to convert heat energy to work by a simple reciprocating motor. A rod of ferromagnetic material is attracted to a magnet and does work against a spring. However at the same time near the magnet it is heated, absorbing heat Q_H , above its Curie temperature (the temperature above which the material becomes paramagnetic) with the result that its moment, \mathcal{M} , becomes smaller. Consequently the force on rod diminishes and it is retracted into the cold zone rejecting heat Q_L into the lower reservoir. Useful work is shown as being merely dissipated in the dashpot.

Thermodynamic analysis can be quickly performed by analysing this heat engine as two adiabatic processes alternated with isothermal processes (fig. 2). The Thermodynamic Identity equates the change in heat to the work around a cycle and thus the area on the T-S diagram is equivalent to multiplying the adiabatic temperature change on magnetisation by the isothermal change in entropy ([12] appendix 1),

$$(\Delta T)_s = -\frac{\mu_0 T}{C_H} \left(\frac{\partial \mathcal{M}}{\partial T} \right)_H \Delta H \quad \text{eqn. 2}$$

$$\Delta S = -\mu_0 \left(\frac{\partial \mathcal{M}}{\partial T} \right)_H \Delta H \quad \text{eqn. 3}$$

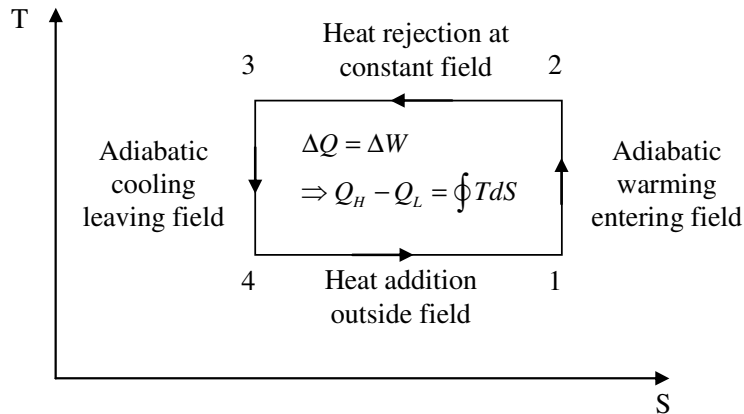
Thus,

$$W = \int_{H_0}^{H_1} \frac{\mu_0 T}{C_H} \left(\frac{\partial \mathcal{M}}{\partial T} \right)_H dH \cdot \int_{H_0}^{H_1} \mu_0 \left(\frac{\partial \mathcal{M}}{\partial T} \right)_H dH \quad \text{eqn. 4}$$

Or approximately,

$$W \approx \frac{\mu_0^2 T}{C_H} \left(\frac{\partial \mathcal{M}}{\partial T} \right)_H^2 (\Delta H)^2 \quad \text{eqn. 5}$$

86 The magneto-caloric effect (MCE) can also be used to refrigerate/pump heat and the MCE
 87 Carnot cycle's TS diagram is just the reverse of figure 2.
 88



89
 90

91 **Figure 3 – T-S diagram MCE Carnot Refrigerator**

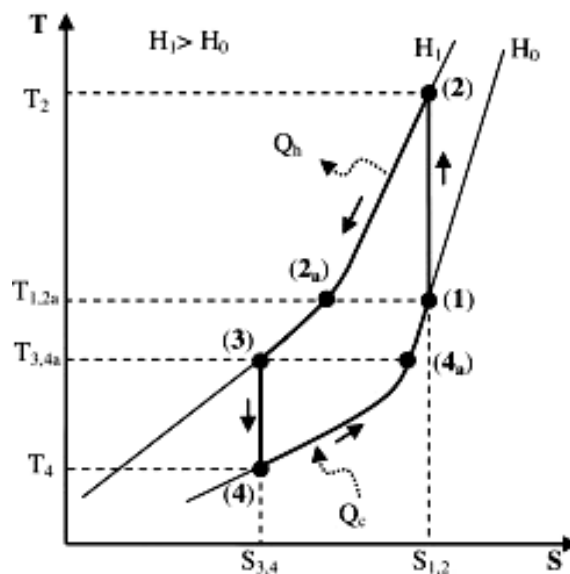
92
 93
 94

95 2.1 The Limitation of MCE Carnot cycles

96

97 The heat engines discussed previously are more practically realised by heat transfer at
 98 constant magnetic intensity in the magnetic analogy of Brayton and Ericsson cycles[13]
 99 (figures 4 and 5). The former cycle performs heat transfer when the magnetic intensity is
 100 higher and thus achieves a higher temperature range and heat transfer between the magneto-
 101 caloric material and the heat transfer fluid. Figure 4 shows this as two adiabatic processes and
 102 two constant intensity processes. Process 2a-3 is an additional cooling caused by a
 103 regenerator that exchanges heat with process 4a-1. The Ericsson cycle heat pump features
 104 isothermal magnetisation and demagnetisation processes with regeneration at processes 2-3
 105 and 4-1. Since the heat exchange process of regeneration in both cases requires a finite
 106 temperature difference, this is an irreversible process and so is a decrease in the efficiency of
 107 both cycles compared to the Carnot cycle.

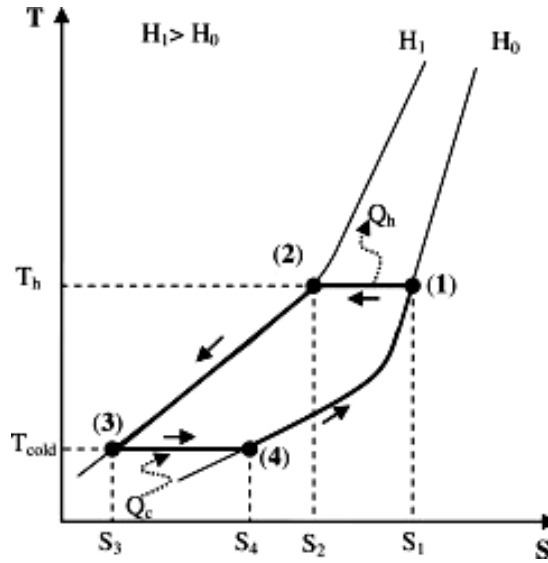
108



109
 110

111 **Figure 4 – Magnetic Brayton cycle**

112



113
114
115

116 **Figure 5 – Magnetic Ericsson cycle**

117

118 Cornwall[12] and Gschneidner et-al[13] go into more detail about cascade Ericsson and the
119 Active Magnetic Regeneration cycle but what is important to the research community is
120 improving the magneto-caloric effect at the core of these cycles. A number of desirable
121 material features are listed[13, 14]:

122

123

124

125

126

127

128

129

130

- Low Debye temperature[15].
- Curie temperature near working temperature.
- Large temperature difference in the vicinity of the phase transition.
- No thermal or magnetic hysteresis to enable high operating frequency and consequently a large cooling effect.
- Low specific heat and high thermal conductivity.
- High electrical resistance to avoid Eddy currents.

131

132

133

134

135

136

137

138

137 **3. Detail on the new Temporary Remanence Cycle**

138

139

140

141

142

143

144

145

146

147

We present now a new type of cycle based upon a feature of so-called super-paramagnetic materials called Temporary Remanence, unused in current heat engines, that has a wide temperature range of operation by being able to boost (eqn. 15) the MCE effect by a phenomenon called “dipole-work” (eqn. 6, Cornwall[12], fig. 9 and sec. 3.3). It is possibly easier to present the cycle first from the kinetic theory viewpoint *then* the thermodynamics viewpoint, whereupon the last presentation will link with the previous discussion about the thermodynamics of conventional MCE engines; we shall see that the arguments flow on logically from convention (eqn. 15). Finally we shall discuss the electro-dynamics of the process, which is mainly a crucial engineering concern.

148
$$W_{dw} = \int_{M,V} \mu_0 M dM \cdot dV = \frac{1}{2} \mu_0 M^2 V \quad \text{eqn. 6}$$

149
 150 This dipole-work leads to an extra term on the thermodynamic identity and is related to the
 151 Faraday Law collapse of the temporary magnetic flux generating power into a resistive load.
 152 This can be made greater than the magnetisation energy input,

153
 154
$$E_{mag} = \int_{M,V} \mu_0 H dM \cdot dV = \mu_0 H M V \quad \text{eqn. 7}$$

155
 156 The difference come from the heat energy converted (secs. 3.1 and 3.2) into work. Thus the
 157 heat engine generates electrical power directly and also cools.

158
 159 In our research we use a stable nanoscopic suspension of magnetic particles in a carrier fluid
 160 called ferrofluid[11]. The particles are so small that they are jostled continuously by the
 161 Brownian motion. As a consequence they on magnetisation display “super-
 162 paramagnetism”[9, 11, 16] which on the spectrum from diamagnetism to anti-
 163 ferro/ferrimagnetism to paramagnetism to ferri/ferromagnetism, displays properties similar to
 164 both paramagnetism and ferri/ferromagnetism: they display no permanent remanence but are
 165 somewhat easy to saturate compared to paramagnets due to their large spin moment.
 166 Temporary remanence is manifest by two mechanisms:

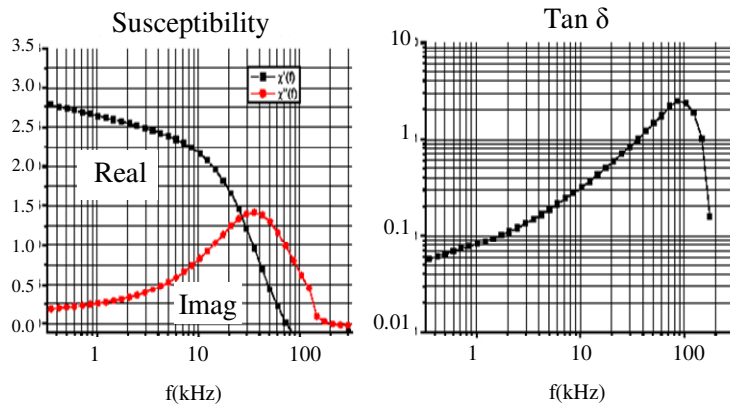
167
 168 Néel:
$$\tau_N = \frac{1}{f_0} e^{\frac{KV}{kT}} \quad \text{eqn. 8}$$

169 And

170 Brownian:
$$\tau_B = \frac{3V\eta_0}{kT} \quad \text{eqn. 9}$$

171
 172 The first relaxation rate can be understood as internal to the ferrofluid particle and involves
 173 lattice vibration and hence it contains the energy term KV related to the crystalline anisotropy
 174 constant and the volume of the particle. The latter is related to the jostling of the particle by
 175 the suspending fluid and contains an energy term related to the viscosity of the suspending
 176 fluid and the volume. Nature uses the principle of least time to determine which dominates
 177 the relaxation rate. Obviously these quantities are amenable to engineering.

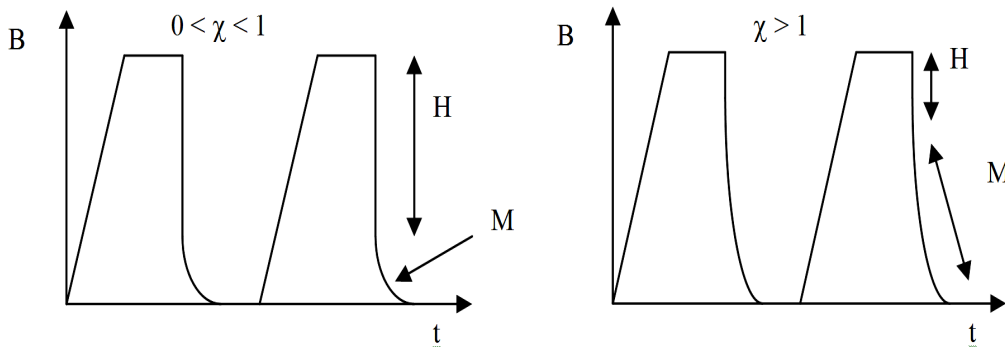
178
 179 Another feature they display on rapid magnetic cycling is hysteresis loss[17, 18]. This is most
 180 pronounced if the rate of magnetisation is comparable to the relaxation rate. The phenomenon
 181 is directly related to the Fluctuation-Dissipation Theorem.[19].
 182



183
184
185
186
187
188
189
190

Figure 6 – Hysteresis loss in typical ferrofluid (Courtesy Sustech GmbH)
LHS Bodé plot in and out-phase components, RHS: Power loss angle

The cycle (called a micro-cycle) is implemented as a magnetising step followed by a de-magnetising step:



191
192
193
194
195

Figure 7 – Micro-cycle magnetising pulses
for $0 < \chi < 1$ and then $\chi > 1$

The figure above shows a train of magnetising pulses for two cases, small and large susceptibility[9]. Observe how the switch-on phase is slow, so that significant hysteresis loss isn't incurred and the switch-off is abrupt to leave a temporary remnant flux (the "Independent Flux Criterion" sec. 3.3.1). Micro-cycles are completed many times a second and result in an adiabatic cooling of the ferrofluid working substance.

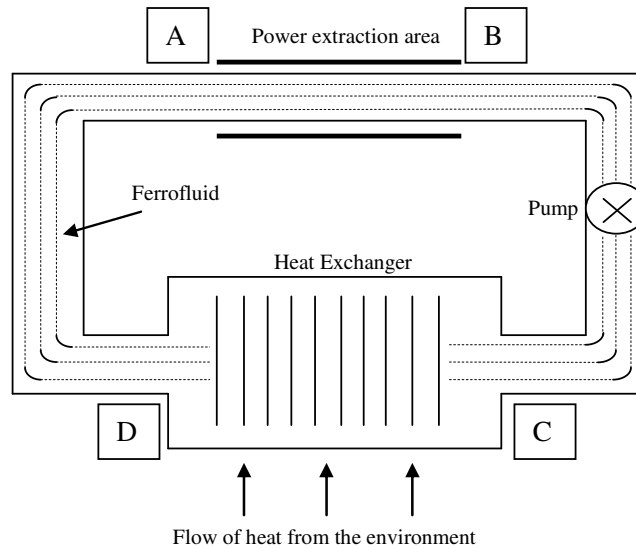
201

To complete the heat engine, the working substance needs to be placed in contact with an external (albeit only one) reservoir. The plant diagram or macro-cycle is depicted in the next figure. In this figure, the micro-cycles happen many times as the working substance transits the "power extraction area" A-B.

206

For the purposes of argument, let us dispel concerns about the pressure-volume work that must be expended circulating the fluid against its tendency to be drawn into the magnetised power extraction area by saying there is a portion of the operation when the magnetising fields are switched off and fluid is simply pumped further around to the heat exchange area C-D.

211



212
213

214 **Figure 8 – Plant Diagram (Macro-cycle)**

215

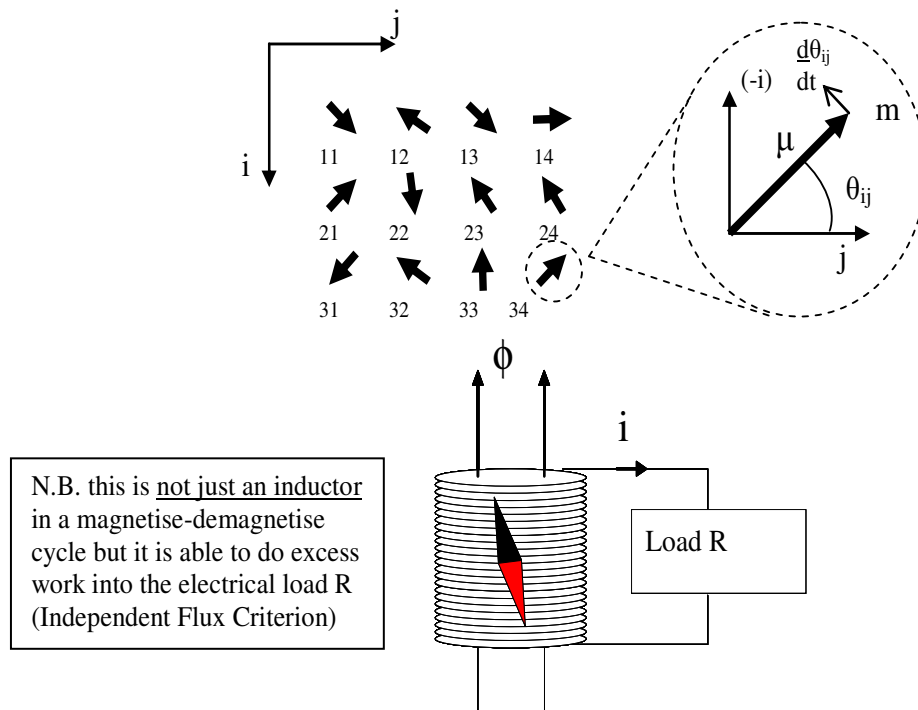
216 We shall develop the theory of the temporary remanence (TR) cycle heat engine by three
217 intersecting analyses: Kinetic Theory, Thermodynamic and Electrodynamic Theories.

218

219 3.1 Kinetic Theory

220

221 In the thesis[12] a lattice of magnetic dipoles is set up to model the ferrofluid (fig. 9).



N.B. this is not just an inductor
 in a magnetise-demagnetise
 cycle but it is able to do excess
 work into the electrical load R
 (Independent Flux Criterion)

222
223

224 **Figure 9 – The Kinetic Theory Model**

225

226

227 The model of dipole-dipole interactions leads to the angular acceleration of each dipole:

228

229

$$\ddot{\theta}_{ij} = \frac{1}{I} \left(-k_{dip} \sum_{\substack{ii=i+1 \\ jj=j+1 \\ ii=i-1 \\ jj=j-1 \\ ii \neq i \wedge jj \neq j}} \tau(\theta_{i,j}, \theta_{ii,jj}, \mathbf{m}, \mathbf{r}) - \mathbf{m}_{ij} \times \mathbf{B}_{ext} \right) \quad \text{eqn. 10}$$

230

231

232 The torque experienced by each dipole is from the external field of the solenoid (\mathbf{B}_{ext}) and the
 233 dipole-dipole interactions resulting from the local fields of its neighbours:

234

$$\tau(\theta_{ij}, \theta_{ii,jj}, \mathbf{m}, \mathbf{r}) = -\mathbf{m}_{ij} \times \overline{\mathbf{B}_{local.neighbour}} \quad \text{eqn. 11}$$

236

237 Taken as a bulk effect, this is of the form $const \times M dM$ or the dipole-work[12] ()

238 where $B = \mu_0 M$

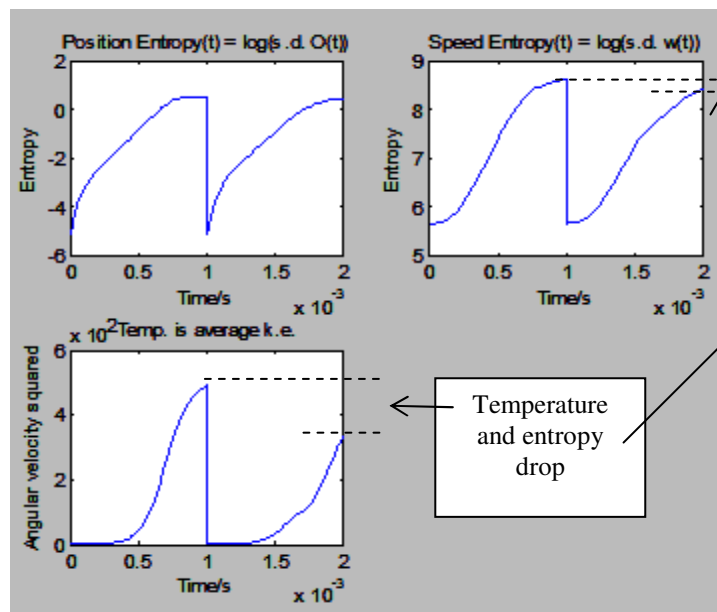
239

240 The model can be run as a molecular dynamics simulation and the author attempted this to
 241 good success, apart from the lack of convergence or *Energy Drift* in these type of simulations
 242 from use of non-symplectic algorithms[20]. It wasn't thought worthwhile to pursue this further
 243 when, as we shall see, analytical solution exists. Nethertheless the entropies of position and
 244 velocity and the temperature are calculated:

245

$$\begin{aligned} S_{pos} &= const \times \ln(\text{standard deviation } \theta_{ij}) \\ S_{vel} &= const \times \ln(\text{standard deviation } \dot{\theta}_{ij}) \\ T &= const \times \text{average}(\dot{\theta}_{ij}^2) \end{aligned} \quad \text{eqn. 12}$$

247



248

249

250 **Figure 10 – Relaxing to equilibrium and then the same but with dipole-work**

251

252 Two simulations were performed, one after the other: In the first simulation the dipoles were
 253 all aligned at the start with zero kinetic energy. The simulation shows this “relaxing” to a
 254 random orientation (the position entropy increases). The potential energy at the start is

255 converted into random kinetic energy (hence the temperature rises as does the velocity
256 entropy).

257
258 The second simulation following right after for comparison models relaxation with dipole-
259 work, that is, the assembly generates electrical work which leaves the system and gets
260 dumped into the resistive load.

261
262 An analytical solution[12] can be obtained by the statistical averaging of the ensemble
263 eqn. 10:

$$264 \overline{I\ddot{\theta}_{ij}} = -k_v m_{ij} \sum_{ii,jj} \frac{\partial}{\partial t} (m_{ii,jj} \cos \theta_{ii,jj}) \sin \theta_{ij} \rightarrow I\ddot{\theta}_{ij} = -k_v (m_{ij} \sin \theta_{ij})^2 \dot{\theta}_{ij} \text{ eqn. 13}$$

266
267 Thus each dipole experiences a drag force (hence proportional to the angular velocity $\dot{\theta}_{ij}$) and
268 slows (hence both temperature and entropy decrease) and this is directly related to the dipole-
269 work (eqn. 11). This shows the mechanism for the transduction of heat energy from the
270 working substance to the electrical load.

271
272 Kinetic Theory/Statistical Mechanics is the source of the Boltzmann expressions in equations
273 8 and 9. Anisotropy can be added to the model (eqn. 10) such that rotation cannot occur
274 unless an energy barrier is exceeded. This has the obvious effect of slowing down the
275 relaxation rate. It is shown ([12] section 2.1.3) that compared to the intrinsic anisotropy
276 energy barrier for the ferrofluid, the additional energy barrier from the dipole-work is entirely
277 negligible, thus kinetically the process of the magnetise-demagnetise TR cycle occurs.

278

279 **3.2 Thermodynamics**

280

281 The relation between Kinetic Theory, Statistical Mechanics and Thermodynamics is close.
282 The first is a low-level description of single microscopic entities acting in concert; the next is
283 a statistical description of a multitude of these low-level equations; finally thermodynamics
284 relates bulk properties to average properties predicted by Statistical Mechanics.

285

286 To be a heat engine, the working substance must first have a property that is a strong function
287 of temperature. This is immediately apparent in equations 8 and 9 with ferrofluid. However
288 with conventional magneto-caloric effect (MCE) engines, focus dwells upon the
289 paramagnetic-ferromagnetic transition and the Curie Point[9, 12]. In the author's thesis a link
290 is made between the TR cycle (figures 7 and 8) and conventional MCE engines by the
291 thermodynamic identity:

292

$$293 dU = TdS + \mu_0 HdM + \mu_0 MdM \text{ eqn. 14}$$

294

295 The last term is the dipole-work such that an amended delta-T equation is derivable by
296 considering 2nd cross-derivatives ([12] section 2.2 and appendix 1) related to the change in
297 magnetising field *and* remnant magnetisation:

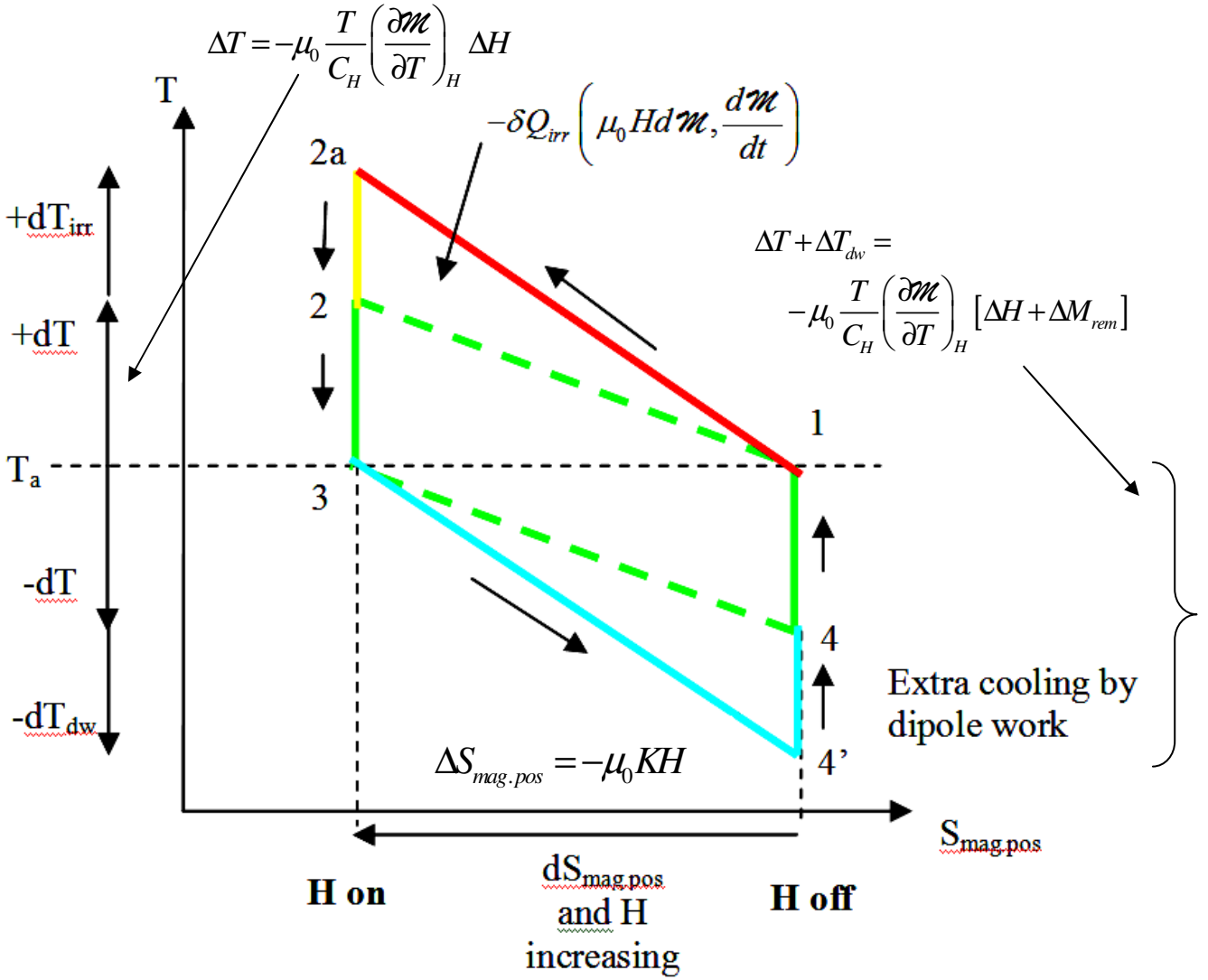
298

$$299 \Delta T = -\mu_0 \frac{T}{C_H} \left(\frac{\partial \mathcal{M}}{\partial T} \right)_H [\Delta H + \Delta M_{rem}] \text{ eqn. 15}$$

300

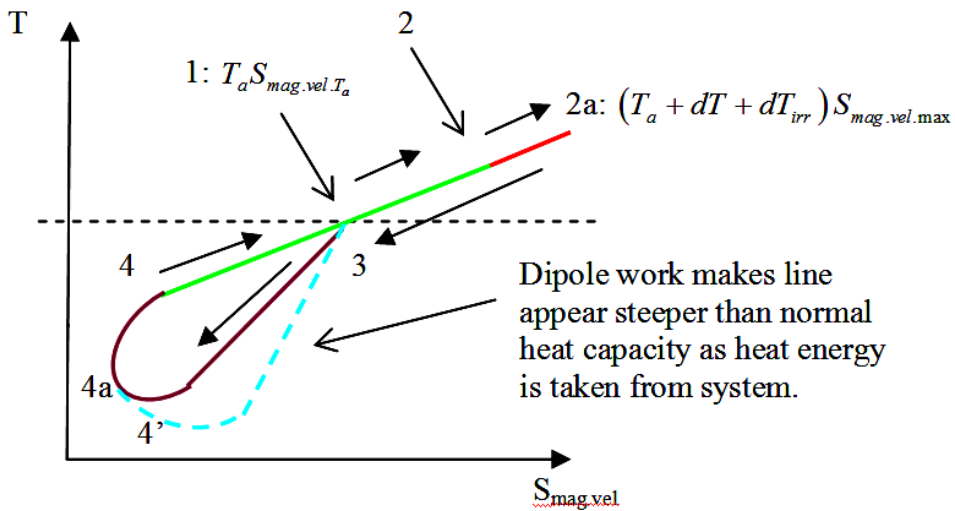
301

302



303
304
305
306
307
308

Figure 11 – Temperature- Positional Entropy Diagram for the micro-cycle



309
310
311
312

Figure 12 – Temperature- Velocity Entropy Diagram for the micro-cycle

313 This shows that, unlike conventional MCE cycles, the TR cycle can operate below the Curie
314 point (so that ΔT on magnetisation from ΔH is negligible) because the magneto-caloric effect
315 occurs from the new dipole-work term in equation 14. Also we point out that, although ΔT is
316 small, the immense surface area of nanoscopic magnetic particles in contact with the
317 ferrofluid carrier liquid ensures massive heat flow ([12] section 2.2.3).

318

319 It is possible to construct ([12] section 2.2.1 to 2.2.4) a temperature-entropy diagram for the
320 micro and macro-cycles (figs. 11 and 12). The figures depict temperature entropy diagrams
321 for an infinitesimal TR cycle. They are somewhat of an abstraction in that the cycle places
322 the magnetic component of the ferrofluid in contact with the carrier fluid at set points in the
323 cycle (2-3) and (4, 4'-1) and considers them thermally isolated for the rest, whereas in reality
324 the magnetic and fluid systems are always in intimate thermal contact. Thermodynamics
325 requires one to construct a series of states with discernable, stable thermodynamic parameters
326 and this is difficult when the system passes through a series of meta-states.

327

328 Figure 11 depicts positional entropy which directly related to magnetic ordering hence the
329 magnetic field of the working substance. The internal cycle represented by numbers 1-4 is the
330 simple MCE in contact with a reservoir. The field switches on between 1 and 2 with the
331 temperature of the working substance raising as the heat capacity is lowered by the
332 magnetising field (the magnetic heat capacity falls and heat is repartitioned to
333 mechanical/kinetic part of the system). Between 2-3 the magnetic system is placed in contact
334 with the ferrofluid carrier liquid which acts as a virtual reservoir and heat is rejected to it.
335 Then between 3-4 the magnetic part, isolated once again, has the magnetising field switched
336 off whereupon the heat capacity rises and heat flows from the mechanical part of the heat
337 capacity to the magnetic part once again such that the magnetic system drops below T_a , the
338 temperature of the carrier fluid. On step 1-4, the magnetic system is placed in contact with the
339 fluid reservoir and heat flows from it to the magnetic system.

340

341 The TR cycle is an adjunct to the reversible MCE cycle in contact with an external reservoir
342 at points 1-2a-2, which represents hysteresis heating of the magnetic component and 3-4'-4,
343 which represents the extra cooling by dipole-work.

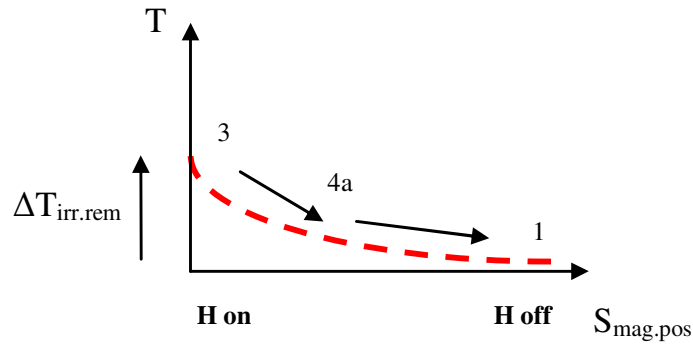
344

345 The step numbers correspond similarly the T-S diagram for the mechanical part of the heat
346 capacity of the magnetic system (fig. 12). We see that it is once again based on the reversible
347 MCE cycle in contact with an external reservoir at steps 1-2-3-4. The difference occurs at
348 point 2-2a with the hysteresis heating (and hence heat transfer between 1-2 on figure 11) and
349 dipole-work cooling 3-4'-4 and heat transfer on figure 11 between 4'-4-1.

350

351 One further point is the conversion of the magnetisation energy (ΔH) into internal energy as the
352 magnetising field is switched off at point 3-4. This is shown as an extra heat input 3-4a-1 in
353 the diagram below and in figure 12 as steps 3-4'-4a-4-1.

354



355
356
357

Figure 13 – The magnetising energy becomes internal energy

358
359
360

The consideration of these diagrams([12] appendices 6 and 7) allows the development of the energy balance equation:

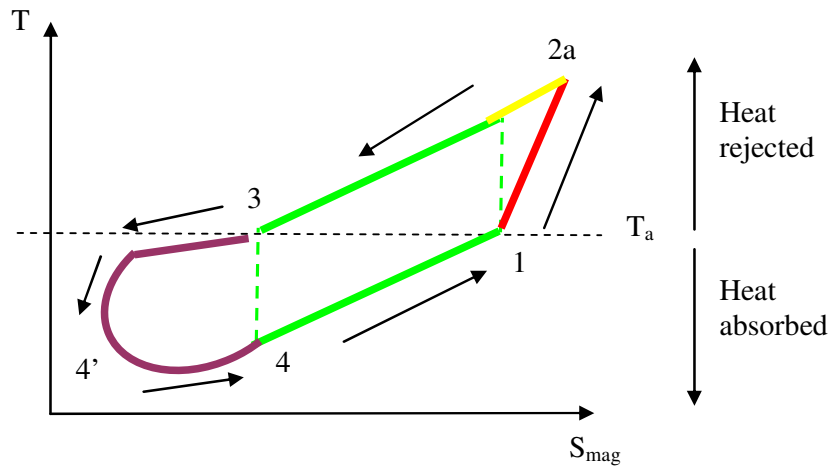
361
362

$$-C_H \frac{d}{dt}(T_{mechanical}) = \frac{d}{dt}(Q_{external}) - \frac{d}{dt}(W) + \frac{d}{dt}(W_{irreversible}) = 0 \quad \text{eqn. 16}$$

363
364

This states the obvious really, that the internal energy is dependent on the heat dumped into the ferrofluid minus the dipole-work. Overall the combined T-S diagram for the positional and mechanical entropies of the working substance is shown in figure 14. Once again, at its core is the reversible MCE cycle 1-2-3-4.

365
366
367
368
369
370
371



372
373
374

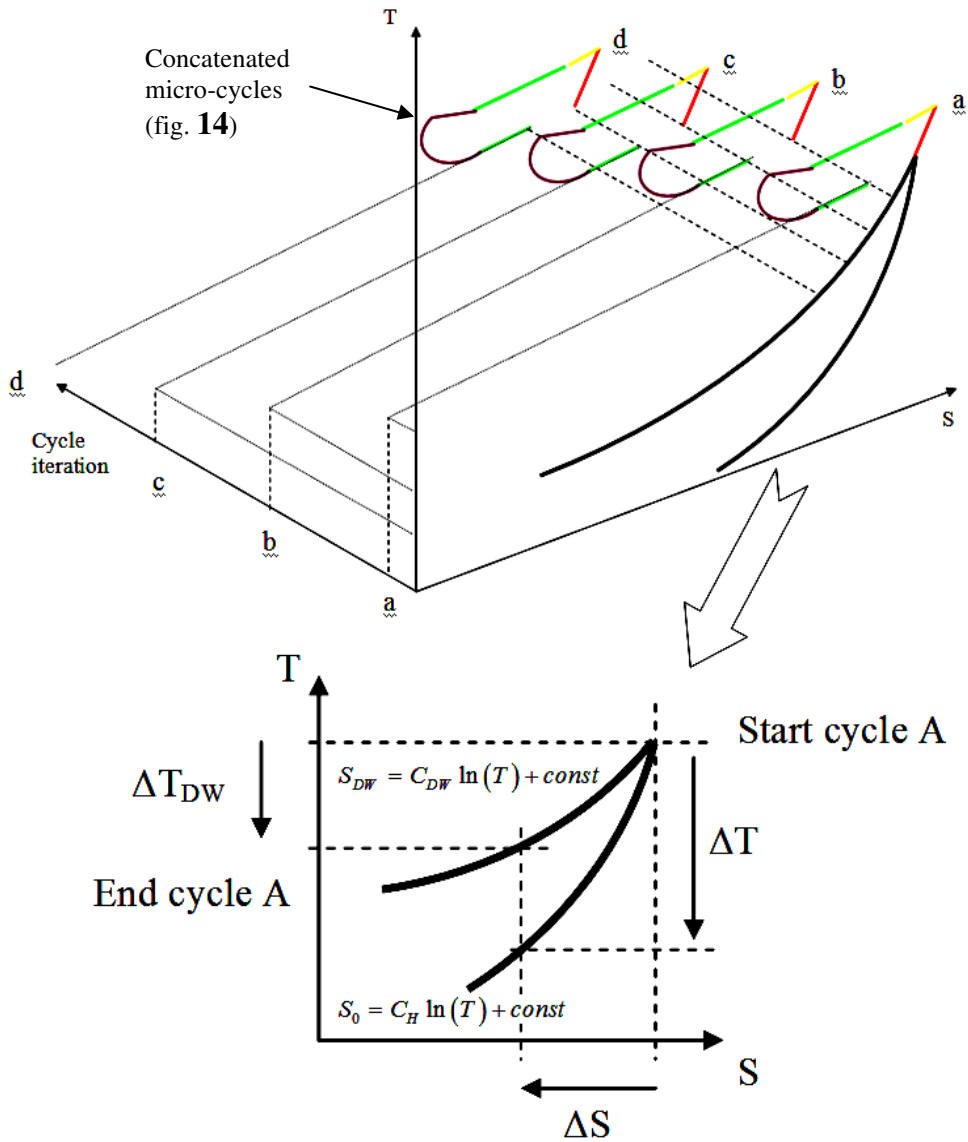
Figure 14 – Temperature-Entropy diagram for the Microcycle

Composed of the positional
and velocity T-S diagrams sub-cycles

375
376
377
378

As mentioned in the discussion about the plant diagram (fig. 8), the macro-cycle is made from many concatenated micro-cycles in the power extraction area. The micro-cycles cause the adiabatic cooling (if we neglect hysteresis heat inputs) of the ferrofluid working substance and we arrive at figure 15 (see [12] section 2.2.4 for original figure).

379
380
381
382
383



384
 385 **Figure 15 – How Micro-cycles relate to the**
 386 **Macro-cycle on a T-S diagram**
 387

388 The 2nd order phase change and the dipole-work in the thermodynamic identity make the
 389 working substance (eqn. 14) seem like another substance (more of this later in the discussion)
 390 with a higher heat capacity. In the lower sub-figure of figure 15 the dipole-work causes a
 391 temperature drop ΔT_{DW} for entropy change ΔS as heat energy leaves the system. If we
 392 reverse our direction and go up the up trace and imagine we are warming the virtual
 393 substance, heat energy not only goes to the working substance but to the external system
 394 because of the dipole-work. In comparison the “native” heat capacity of the working
 395 substance without the dipole work in lower trace of the sub-figure is:
 396

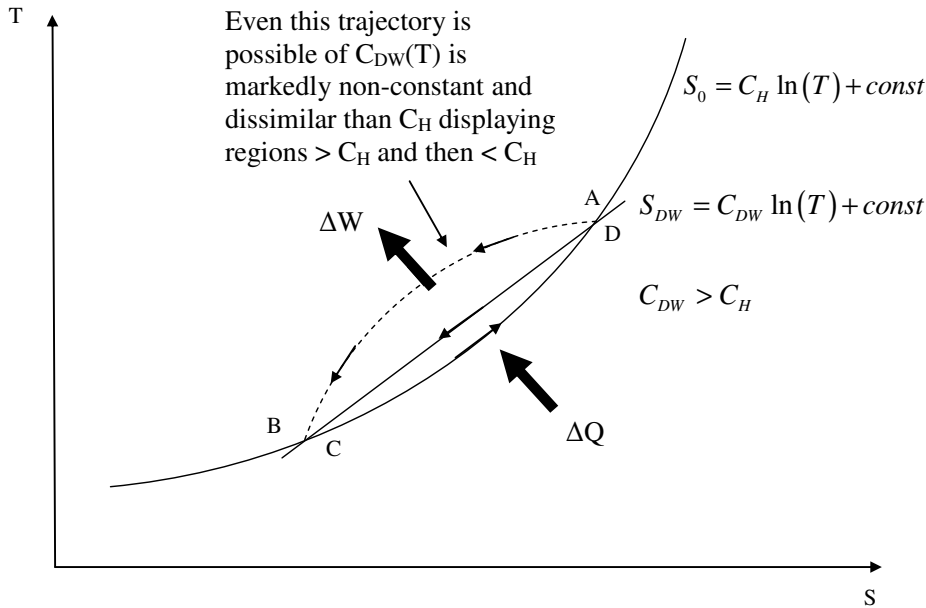
397
$$S_0 = C_H \ln(T) + const \quad \text{eqn. 17}$$

398
 399 The upper trace has an higher virtual heat capacity:
 400

401
$$S_{DW} = C_{DW} \ln(T) + const \quad \text{eqn. 18}$$

402

403 Zooming out from the upper sub-figure of figure 15 we arrive at the macro-cycle T-S
 404 diagram and then relate that to the plant diagram of figure 8 by the labels A-B-C-D:
 405



406
 407

408 **Figure 16 – Macro-cycle T-S diagram related to points on plant diagram**

409
 410
 411
 412
 413

The area between the two trajectories of heat capacity C_H (eqn. 17) and C_{DW} (eqn. 18) is the heat absorbed at the heat exchanger and converted into electrical energy in the power extraction zone.

414 3.3 Electrodynamics

415
 416
 417
 418
 419
 420
 421

The Kinetic Theory and Thermodynamic analysis of the previous section have laid the groundwork for the TR cycle. It would seem a simple matter of Faraday/Lenz law collapse of the remnant flux in to a coil attached to an electrical load to deliver the goods of heat energy conversion, as depicted in figure 9. However there is some subtlety in the explanation of the demagnetisation step and a final electrical method to deliver excess power.

422 3.3.1. Not “just an inductor”

423
 424
 425
 426
 427
 428
 429

The lower sub-figure in figure 9 and the magnetise-de-magnetise cycle creates the impression that the setup is just a simple electrical circuit and if anything, should act as a dissipative sink of energy due to hysteresis losses. We show that this is not so and that excess electrical energy can enter the circuit from an external source of mechanical “shaft-work”, effectively rotating the source of the magnetic flux inside the coil.

430
 431

Firstly we consider the net electrical work around a magnetisation, de-magnetisation cycle.

432

$$\oint v i dt = -\oint \frac{d\lambda}{dt} i dt \quad \text{eqn. 19}$$

433
 434
 435

Where λ is the flux linkage. Integrating the RHS by parts:

$$\oint i(t) \frac{d\lambda(t)}{dt} dt = \left[i(t)\lambda(t) - \int \lambda(t) \frac{di(t)}{dt} dt \right]_{0^+}^{0^-} \quad \text{eqn. 20}$$

$$= i(0^-)\lambda(0^-) - i(0^+)\lambda(0^+) - F(\lambda(0^-), i(0^-)) + F(\lambda(0^+), i(0^+))$$

437

438 Where F(..) is the integrand of the parts term. Now, since $i(0^+) = i(0^-)$ and $\lambda(0^+) = \lambda(0^-)$ the
 439 first two terms cancel. Let a dependent flux be represented by,

440

$$i(t) = g(\lambda(t)) \quad \text{eqn. 21}$$

442

443 Where g is an arbitrary function. The second integral of eqn. 20 can be integrated by parts a
 444 second time by applying the chain rule:

445

$$\int \lambda(t) \frac{di(t)}{dt} dt = \int \lambda(t) \frac{dg(\lambda(t))}{d\lambda(t)} \frac{d\lambda(t)}{dt} dt \quad \text{eqn. 22}$$

447

448 Thus,

$$\oint \lambda(t) \frac{dg(\lambda(t))}{d\lambda(t)} d\lambda(t) = \left[\lambda(t)g(\lambda(t)) - \int g(\lambda(t)) \cdot 1 \cdot d\lambda(t) \right]_{0^+}^{0^-} \quad \text{eqn. 23}$$

$$\Rightarrow G(\lambda(0^+)) - G(\lambda(0^-)) = 0$$

450

451 The first term on the RHS cancels due to the flux being the same at the start and end of the
 452 cycle. The integrand on the RHS cancels for the same reason. The above result shows that a
 453 dependent flux (eqn. 21) cannot lead to net power. The proof sheds more light on the
 454 necessary condition for an independent flux: *the flux is constant for any current including*
 455 *zero current* – it bares no relation to the modulations of the current. The proof also dispels
 456 any form of dependent relation, non-linear or even a delayed effect. If equation 21 was
 457 $i(t) = g(\varphi(t - n))$ this could be expanded as a Taylor series about $g(\varphi(t))$ but there would still
 458 be a relation, the flux would still be dependent.

459

460 Thus it is a statement of the obvious (the First Law of Thermodynamics) that excess power
 461 production in an electrical circuit cannot happen by electrical means alone; flux changes must
 462 happen by some outside agency such as electro-mechanical shaft-work to cause energy
 463 transduction.

464

465 In regard to the Kinetic Theory section and figure 9, we are drawing an analogy with the
 466 microscopic dipoles rotating via the randomisation process and the “micro-shaftwork” of heat
 467 energy. In fact, considering the energy of a dipole in a field[5-7]:

468

$$E = +\mathcal{M} \cdot \mathbf{B} + const \quad \text{eqn. 24}$$

470

471 It matters not whether the magnetic moment is rotated wholesale or randomised between the
 472 maximum and minimum energy configuration, it is the same result:

473

$$\Delta E \Big|_{\max}^{\min} = \mathcal{M} B \cos \theta \Big|_0^{\pi/2} \text{ or } \mathcal{M} \Big|_{\mu_{\max}}^0 B \cos \theta \quad \text{eqn. 25}$$

475

3.3.2. Simple resistive load returns less than the input magnetisation energy

We can model the electrodynamics of the de-magnetisation step into a resistive load by a set of state equations[12]:

$$\frac{dM}{dt} = -\frac{1}{\tau}(M - \chi\mu_r H) \quad \text{eqn. 26}$$

$$-\frac{d\lambda}{dt} - iR = 0 \quad \text{eqn. 27}$$

Where,

$$H = \frac{N}{D}i \quad \text{eqn. 28}$$

And

$$\lambda = NAB \Rightarrow NA\mu_0\mu_r (H + M) \quad \text{eqn. 29}$$

Equation 26 represents very accurately[9, 11, 17, 18] the dynamics of the ferrofluid to a magnetising field, H^\dagger . The “effective susceptibility” $\chi\mu_r$ is just the product of the susceptibility and the relative permeability of a co-material placed intimately in contact with it. This is just an engineering feature for easier design.

The author then solves the set of equations in the s-domain[12] for the current as $R \rightarrow 0$:

$$i(t) = \frac{DM_0}{N} e^{-t/\tau'_{ferro}} = \frac{DM_0}{N} e^{-tR/L(1+\mu_r\chi)} \quad \text{eqn. 30}$$

And calculates the ultimate electrical work delivered to the load:

$$\int_0^\infty i^2(t) R dt \Rightarrow W_{dw.L/R \rightarrow \infty} = \frac{1}{2} \frac{\mu_0}{(1 + \chi\mu_r)} M^2 V \quad \text{eqn. 31}$$

The work done magnetising is given by: $\int H dB \cdot dV$ of which the “H” field energy is discarded, as this can be returned with total efficiency if done by a mechanical magnetisation process or very nearly so with an electronic process ([12] sec. 3.2), leaving:

$$\int_{M,V} \mu_0\mu_r H dM \cdot dV = \mu_0 H M \dot{V}$$

The integrand has been resolved with the relative permeability of the material in close proximity to the working substance (the “co-material”) subsumed into M' . We can further write the integrand by $M' = \mu_r \chi H$ as (dropping the primes):

[†] Feynman in his lecture notes is quite scathing about the term “H-field” which is used by electrical engineers and those working in the magnetics of materials,

“... there is only ever B-field, the magnetic field density ... it is a mathematical arrangement to make the equations of magneto-statics come out like electro-statics when we know isolated magnetic poles don't exist by Maxwell's Equations, $\text{div } B = 0$.”

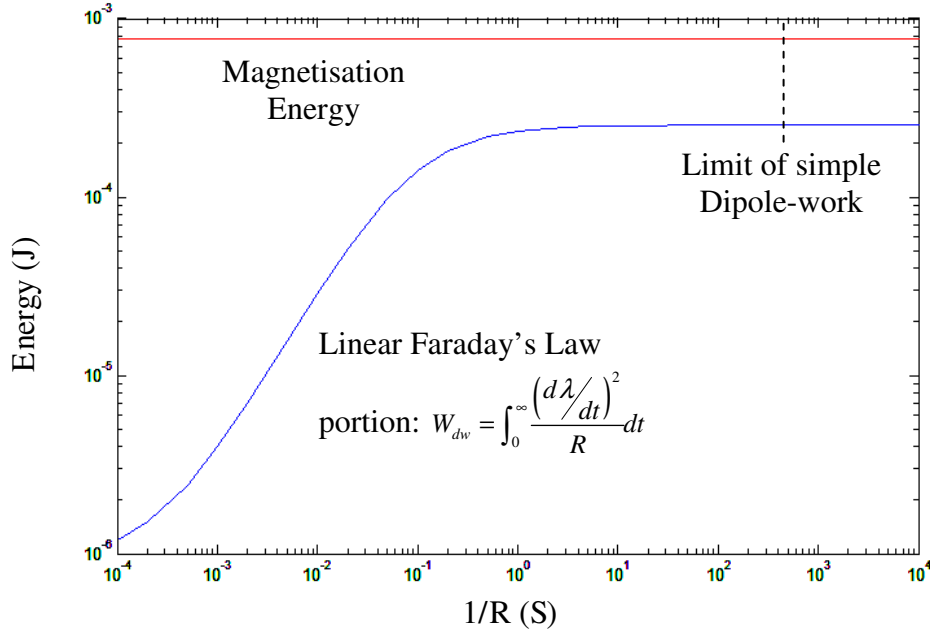
510

$$E_{mag} = \frac{\mu_0}{\chi\mu_r} M^2 V \quad \text{eqn. 32}$$

511

512 The dynamical equations can be simulated (or indeed plotted by experiment[12]) and the
 513 electrical work plotted against 1/R:

514



515

516

517 **Figure 17 – Magnetisation Energy always exceeds simple dipole-work into resistive load**

518

519 For the simple arrangement of coil with decaying ferrofluid flux into a resistive load depicted
 520 in the lower sub-figure of figure 9, the magnetisation energy input will always exceed the
 521 electrical work output. How to circumvent this is discussed in the next section.

522

523 **3.3.3. The “H-field” cancellation method**

524

525 The source of the problem for the returned electrical work being less than the magnetisation
 526 energy is from the slowing of the current waveforms as the electrical load tends to zero:

527

528 In the s-domain, the current is:

529

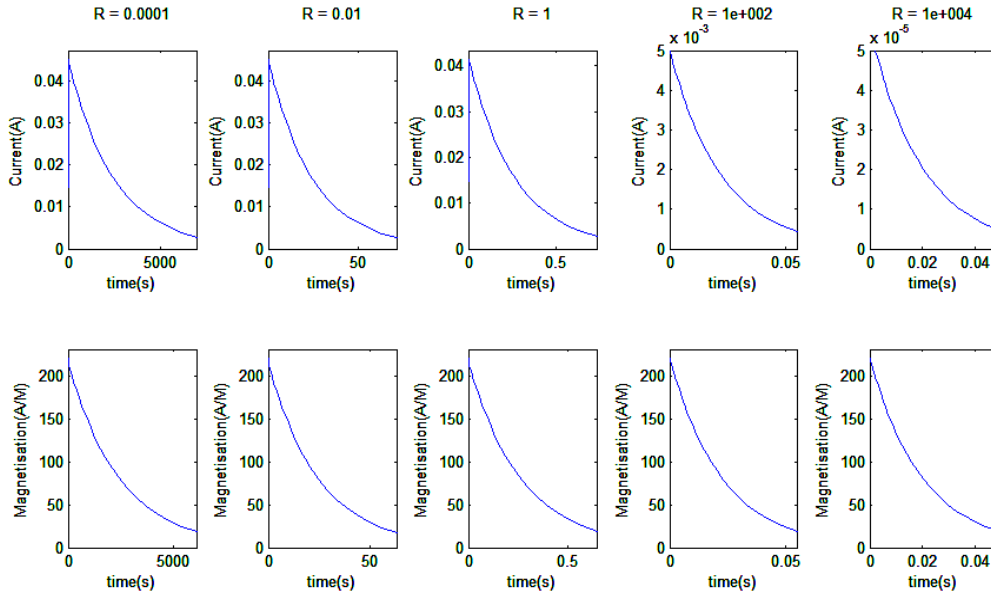
$$I(s) = \frac{\frac{DM_0}{N}}{s^2 \tau_{ferro} + s \left(\frac{R}{L} \tau_{ferro} + (1 + \mu_r \chi) \right) + \frac{R}{L}} \quad \text{eqn. 33}$$

531

532 The dominant pole of this function shows that the time constant tends to a function purely of
 533 the circuit inductance and resistance:

534

$$s \cong \frac{c}{b} \Rightarrow -\frac{1}{\tau'_{ferro}} = -\frac{1}{\tau_{ferro} + \frac{L(1 + \mu_r \chi)}{R}} \quad \text{eqn. 34}$$



536
537

538 **Figure 18 – The slowing current and magnetisation waveforms with lower resistance**
539 **electrical load**

540
541

542 The way around this is to strike out the re-magnetising H-field[7, 8] in equation 26:

543

$$\frac{dM}{dt} = -\frac{1}{\tau} (M - \chi\mu_r H)$$

544

545

546 Whereupon new current dynamics result:

547

$$I(s) = \frac{\frac{DM_0}{N}}{s^2 \tau_{ferro} + s \frac{R}{L} \tau_{ferro} + \frac{R}{L}} \quad \text{eqn. 35}$$

548

549

550

551 The current in the time domain in the limit $R \rightarrow 0$ is,

552

$$i(t) = \frac{DM_0}{N} e^{-t/\tau_{ferro}} = \frac{DM_0}{N} e^{-tR/L} \quad \text{eqn. 36}$$

553

554

555 And then the dipole-work limit by the cancellation method is obtained by $\int_0^{\infty} i^2(t) R dt$ once

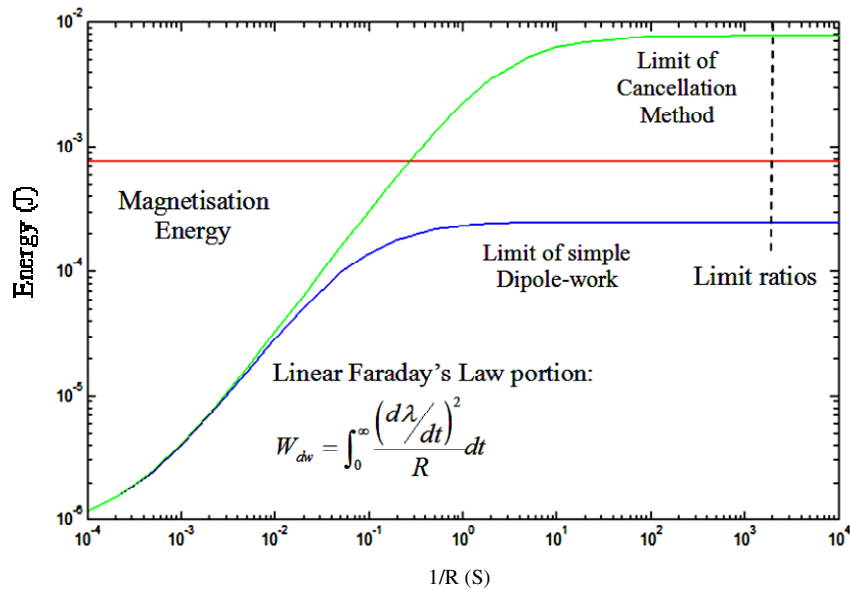
556 again:

557

$$W_{dw.cancel.L/R \rightarrow \infty} = \frac{1}{2} \mu_0 M^2 V \quad \text{eqn. 37}$$

558

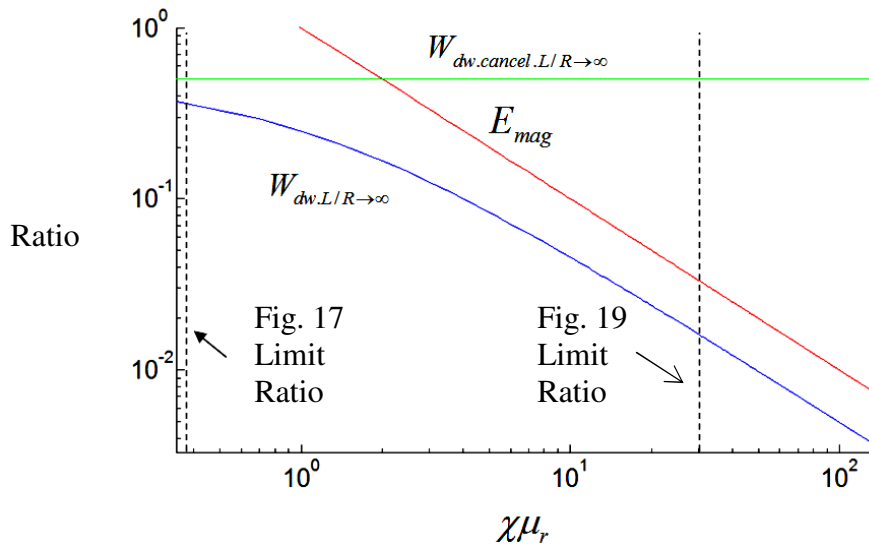
559 This is seen to be the magnetic field energy of the ferrofluid flux and is greater than the input
 560 magnetising energy, equation 32. Simulating the dynamic equations with the approach[12]
 561 one can plot and obtain the graph below for one set of parameters $\chi\mu_r \sim 30$:
 562



563
 564
 565
 566
 567
 568
 569
 570
 571

Figure 19 – Dipole-work exceeding magnetisation energy by the H-field cancellation method

We can plot the variation in the limit ratios of the simple dipole-work, the magnetisation energy and the dipole-work with the cancellation method versus parameter $\chi\mu_r$, by taking the ratio of equations 31, 32 and 37:



572
 573
 574
 575
 576
 577
 578
 579

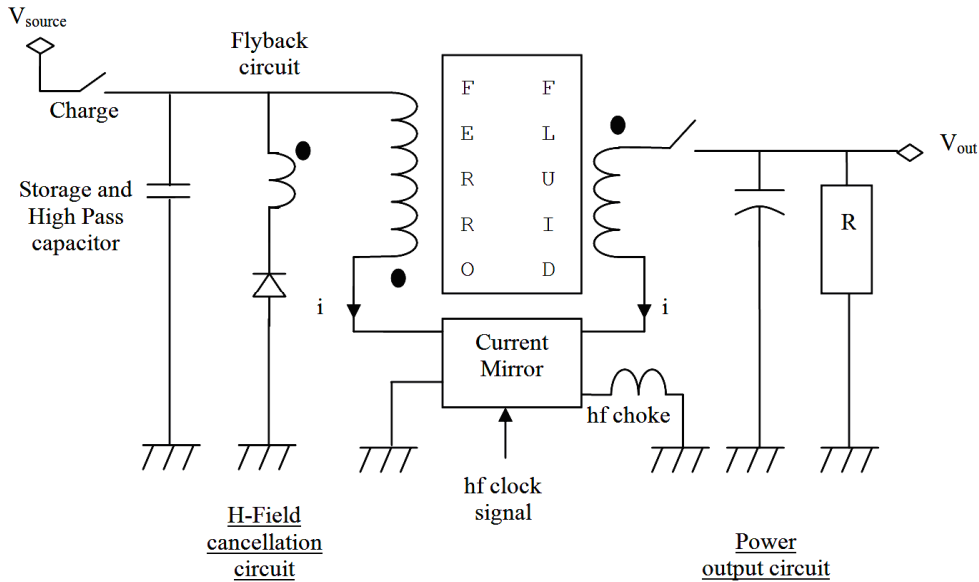
Figure 20 – Variation of parameter $\chi\mu_r$

For all variation of parameters, the magnetisation energy is always greater than the dipole-work without the cancellation method. However if $\chi\mu_r > 2$ the dipole-work, with the cancellation method, will exceed the magnetisation energy input. The power produced by the device is then:

580
581
582
583
584
585

$$P = (W_{dw.cancel} - E_{mag} - W_{losses}) F_{cycle}$$

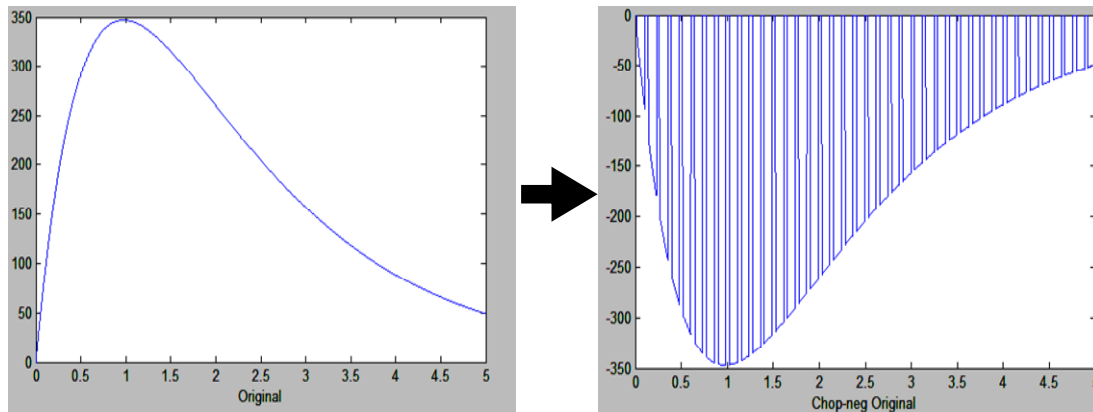
Confirming what was said in the thermodynamic section and equation 16.
The circuit to perform the cancellation method is shown below and detailed description of its mechanism of action can be found in the thesis ([12], sec. 4.3).



586
587
588
589
590
591
592

Figure 21 – The H-Field Cancellation Scheme (LHS circuit)

The circuit works by sampling the current in the power circuit (RHS) and makes a “chopped” proportional copy of it.

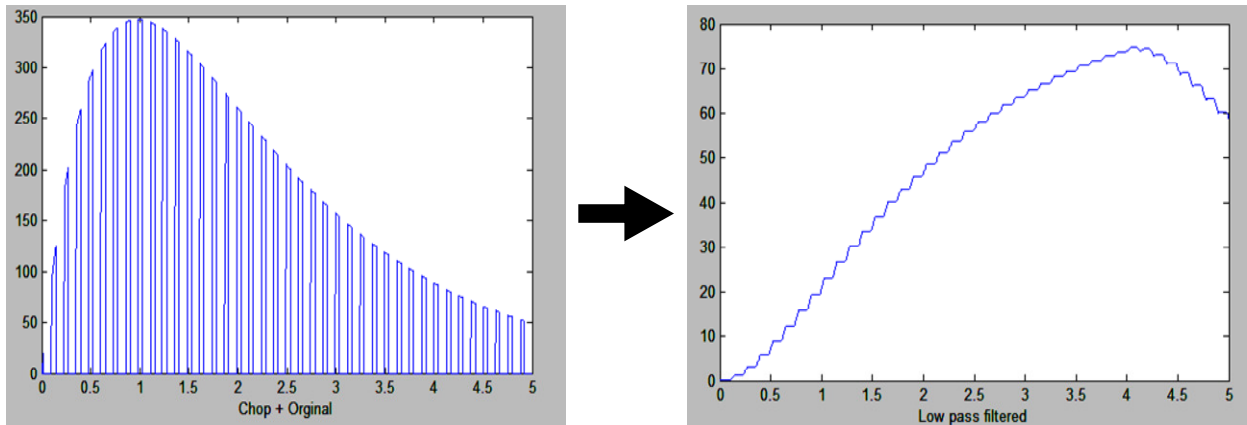


593
594
595
596
597
598
599
600

Figure 22 – Sampling, inverting and “chopping” the current/H-field

The LHS then generates its own H-field which sums with the RHS. The ferrofluid naturally low-pass filters this resultant H-field because of its high harmonics and even more so at very high frequency where the ferrofluid will not exhibit a response nor dissipation (fig. 6). One can observe how the resulting H-field is reduced in the rightmost figure.

601



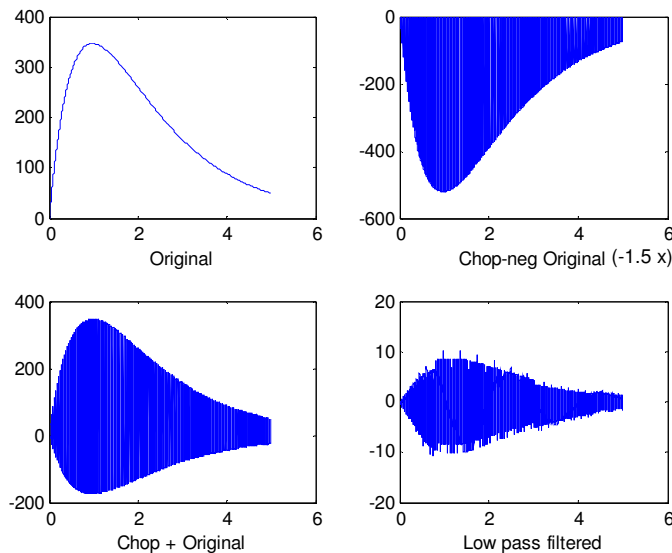
602

603

604 **Figure 23 – The resultant high frequency H-field gets low-pass filtered**

605

606 Even better cancellation comes from asymmetric summation of the inverted, chopped field to
607 the magnetising field. Below is shown the result of summing $-1.5 \times$ the original field:
608



609

610

611 **Figure 24 – Asymmetric sampling and summation**

612

613 The author analyses the electrical work required to operate the H-field cancellation scheme
614 ([12], sec. 4.3.1) and notes that by the inclusion of filtering elements and the “flyback”
615 circuitry, that the LHS circuit only does work establishing the cancellation field and this can
616 be done with high efficiency in a regenerative manner.

617

618 **3.4 Summary of the Temporary Remanence cycle**

619

620 This section on the analysis of the Temporary Remnant cycle is built on the foundations of
621 Kinetic Theory, Thermodynamics, Electrodynamics and experiment.

622

623 Kinetic Theory shows that the relaxing magnetic field acts as a velocity damping term to each
624 magnetic particle undergoing Brownian motion. The electromagnetic field couples to the
625 thermal system, the electromagnetic system then couples to the external electrical system to
626 which power is transferred.

627 Thermodynamics shows:

628

629 ▪ A “delta T”, a change in temperature of the working substance from the magnetic
630 work related to the magnetic properties of the material.

631

632 ▪ On considering the magnetic enthalpy[12], a new term “MdM” called the dipole-work
633 is added onto the thermodynamic identity and is only relevant when heat transfer
634 occurs. This happens on the second half of the Temporary Remanence cycle. This ties
635 in with the Kinetic Theory where MdM is the velocity damping term.

636

637 ▪ T-S diagrams show how the entropies of the magnetic system form a heat engine.
638 Tying in with Kinetic Theory, once again, the variation in entropy associated with the
639 velocity distribution of the magnetic particles is the source of the heat transference.

640

641 ▪ An energy balance equation that shows how the internal energy of the working
642 substance falls with electrical work it performs.

643

644 Electrodynamics shows:

645

646 ▪ The dynamics of the electrical generation process.

647

648 ▪ The work delivered to an electrical load by Faraday/Lenz/Maxwell induction law and
649 that this is of the form MdM, once again.

650

651 ▪ The work delivered to an electrical load with the field cancellation technique and that
652 this exceeds the input magnetisation energy substantially. The difference comes from
653 the conversion of heat energy to electrical energy.

654

655 Cornwall[12] (2.2.3) shows that power densities at least around 1MW per $1\text{m}^3/\text{s}$ flow-rate are
656 possible with the technique and this is comparable to existing heat engines and heat pumps,
657 though high efficiency and few moving parts.

658

659 **4. Analytical proof that phase change engines can be** 660 **Maxwell Demons**

661

662 Should we be so scared by the concept of type 2 perpetual motion? We already know that
663 heat energy *is* microscopic perpetual motion with the continual exchange of kinetic to
664 potential energy; two-body simple harmonic oscillation does this and we might extend the
665 notion and call it “n-body complicated oscillation”. Clearly our Maxwell Demon is part of the
666 n-body complicated oscillatory dynamics of the system and we should find the law,
667 mechanism or rationale providing the underlying reason why this is possible.

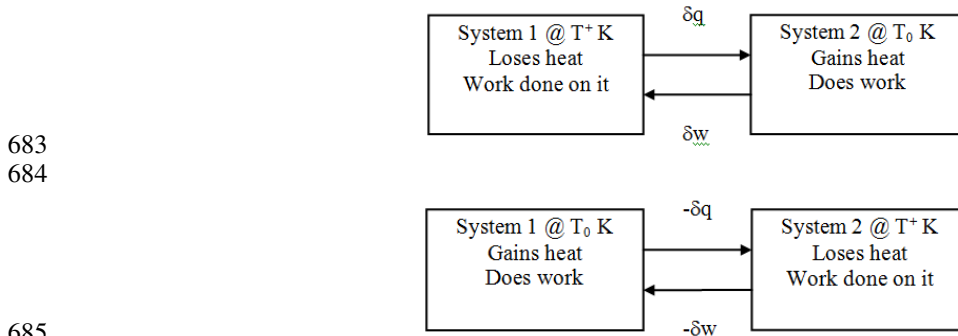
668

669 If one deals with microscopic fluxes at equilibrium, one can say that an exceedingly large
670 amount of *microscopic work* can occur at *constant temperature*, as this clearly is how
671 individual particles rise in potential at equilibrium. There is no conflict with the Carnot result
672 if one takes this viewpoint, that as $T_H - T_C \rightarrow 0$, the efficiency η tends to zero,

673

674
$$\frac{\Delta W}{\Delta Q_H} = \eta = \left(\frac{T_H - T_C}{T_H} \right)$$

675
 676 We argue that the microscopic work-flows at constant temperature become essentially
 677 limitless based on the microscopic heat-flows, which are essentially limitless too. All we are
 678 saying is that if the micro-flow of heat, δQ is exceedingly large near (or approaching near)
 679 constant temperature, then even if η is not quite zero, the work-flows will be large like the
 680 microscopic heat-flows too. This is guaranteed by the statistical fluctuation of temperature at
 681 equilibrium[15, 19], figure 25.
 682



687 **Figure 25 – Statistical fluctuation in temperature with micro-heat and micro-work flows**

688
 689 We are now in a position to see why phase change is key to making a Maxwell Demon. At
 690 equilibrium between two phases, microscopic fluctuations in temperature effectively form
 691 microscopic heat engines that are able to do work against the phase boundary.
 692

693 Lemma: Constant Temperature

694
 695 At constant temperature microscopic heat and work are available and can partition energy
 696 across a phase boundary.
 697

698 So if a *microscopic* demon is possible how is a *macroscopic* demon made?
 699

700 Lemma: Phase Transition Sorting

701
 702 Macroscopic work is obtainable from microscopic work processes at constant temperature
 703 by the working substance undergoing a phase transition.
 704

705 By definition, a phase is a macroscopic representation of underlying microscopic properties.
 706 In a sense, the phase change has “magnified” the microscopic demon.
 707

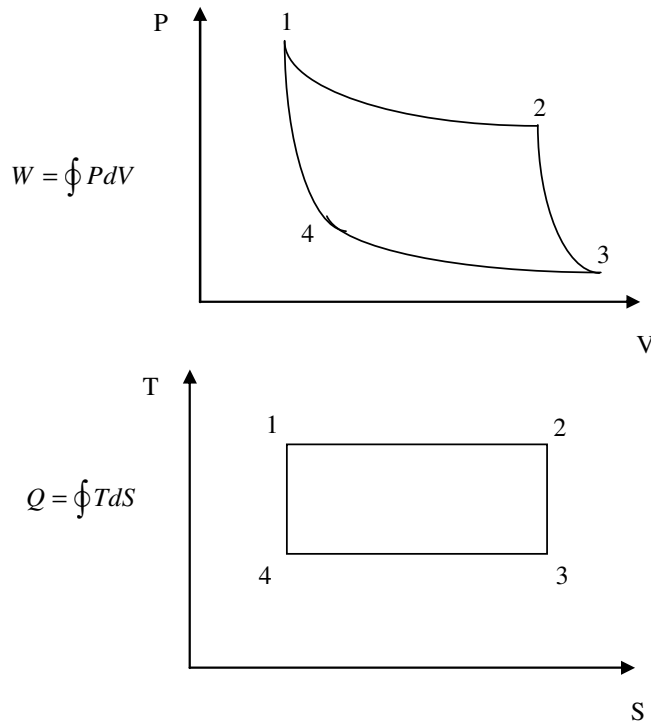
708 This can be understood from the thermodynamic identity:
 709

710
$$dU = TdS - PdV + \mu(P, T, \phi)$$

711
 712 Where ϕ is a potential function of position.
 713

714 Since dU is an exact integral, any means of cycling the working substance by any of the
 715 variables of the system will not produce excess energy from the lowering of the internal

716 energy of the working substance. Let us understand this more by reviewing a conventional
 717 Carnot engine.
 718



719

720 **Figure 26 – PV and TS diagrams for Carnot Engine**
 721

722
 723 The working substance being only one material is constrained to traverse fixed trajectories in
 724 PV or TS space. The familiar alternating of isothermals with adiabatics is required to map out
 725 an area, as moving reversibly along 1-2: isothermal-adiabatic or 1-2-3: isothermal-adiabatic-
 726 isothermal, will not return to the starting co-ordinates. The last step maps out an area so that:
 727

$$\Delta U = \Delta Q - \Delta W = 0$$

728

$$\Rightarrow \Delta W = \Delta Q$$

729

730 This cannot be done with just one reservoir and the last step 3-4 must come into contact with
 731 the lower reservoir. Consider now the meaning of the chemical potential, it is the
 732 thermodynamic potential per particle:

733

$$du = Tds - pdV + \mu \tag{eqn. 38}$$

735

736 Lower case indicates that this is per particle. The chemical potential has two parts, the
 737 internal and external[10]. If at some point in a thermodynamic cycle an external
 738 potential μ_{ext} is added or changed then the thermodynamic identity can be made inexact,

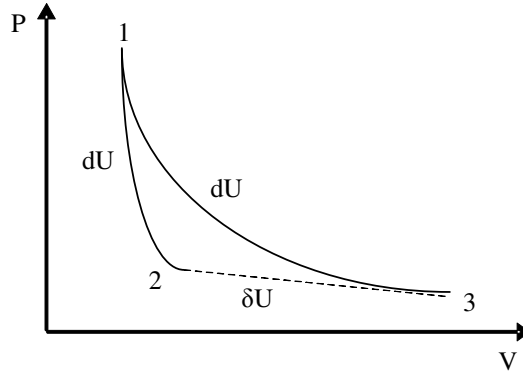
739

$$\delta u = Tds - pdV + \mu_{int} + \mu_{ext} \tag{eqn. 39}$$

740

741
 742 A change of μ by external potential can only correspond to a phase change as this will
 743 introduce potential energy terms, such as that pertaining to latent heat or new magnetisation

744 energy terms, for instance i.e. dipole-work (eqn. 14). It is as though we have a different
 745 working substance not constrained to the trajectories of one substance in PV or TS space and
 746 we can achieve net work from only one reservoir. For instance, in the hypothetical PV
 747 diagram shown below, the working substance might expand adiabatically from 1-2, undergo a
 748 phase change and do work 2-3 and then be placed back in contact with the one reservoir 3-1.
 749



750
 751 **Figure 27 – Illustrative PV diagram**

752
 753 These considerations are not unlike the TS diagrams in figures 14 and 16.
 754

755 5. What is an heat engine?

756
 757 An engine or machine is understood to be a device that transforms one form of energy into
 758 another, usually mechanical energy. An heat engine is then one which a substantial change in
 759 its entropy that is intrinsic to its operation. Thus a charged capacitor discharging into an
 760 electric motor is an engine but not an heat engine; although there is a change in chemical
 761 potential of the electrons constituting the current, it operates at high efficiency and a little of
 762 the electrical energy is converted to heat, the device can operate, in the limit (using
 763 superconductors, etc.) of turning all the electrical energy into mechanical energy. Let us see
 764 how this is so:

765

$$dU = TdS - PdV + Fdx + \sum_{i=1}^n \mu_i dN_i$$

766
 767 Where we have included a generalised force term and generalised displacement Fdx . Then
 768 we note that entropy is a property of the system and an exact differential:
 769

770

$$\Delta S = \int_{T_0}^T \left(\frac{\partial S}{\partial T} \right)_{V,x,N_i} dT + \int_{V_0}^V \left(\frac{\partial S}{\partial V} \right)_{T,x,N_i} dV + \int_{x_0}^x \left(\frac{\partial S}{\partial x} \right)_{T,V,N_i} dx + \sum_{i=0}^n \int_{N_{0,i}}^{N_i} \left(\frac{\partial S}{\partial N_i} \right)_{T,V,x} dN_i$$

771 eqn. 40
 772

773 It is possible for some types of engine to proceed from a starting to an end state with little

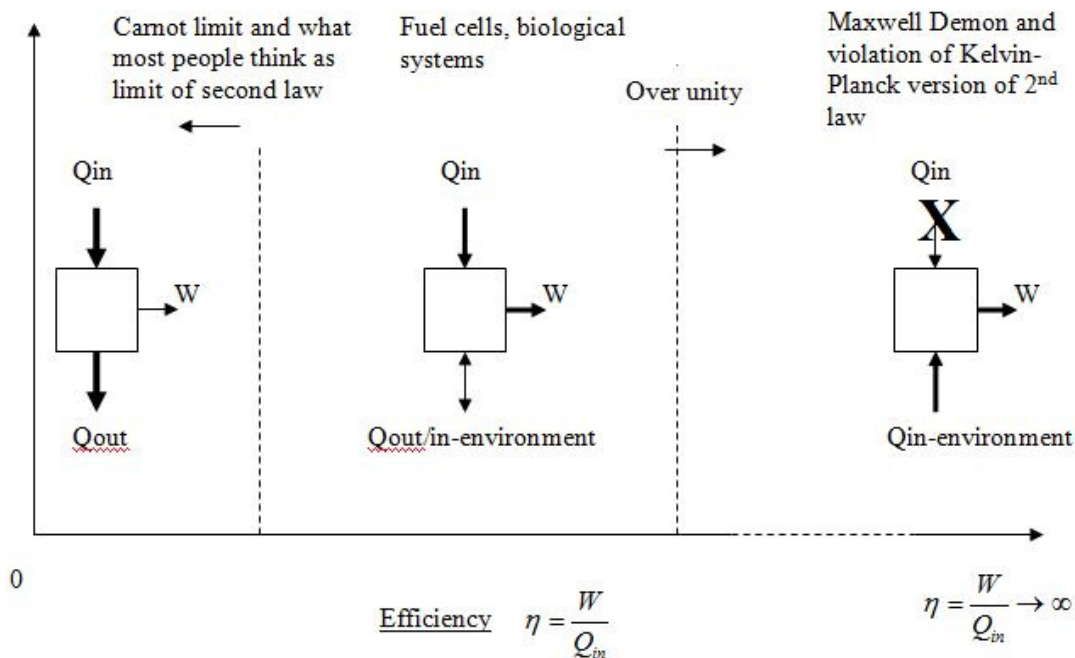
774 variation in T, V and also $\left(\frac{\partial S}{\partial x} \right)_{T,V,N_i}$ or $\left(\frac{\partial S}{\partial N_i} \right)_{T,V,x}$ such that the generalised work term

775 responds to the changes in the chemical potential. In other words, the energy conversion is
 776 very efficient. This is the case with our capacitor-motor analogy or indeed, an hydro-electric
 777 dam. The chemical potential of water in a dam or electrons in a charged capacitor will have a

778 potential term from gravity Mgh or the electric field QV , respectively but this doesn't affect
 779 the entropy before or after the process.

780
 781 However for the type of cycle or process where it is part-and-parcel of the operation that
 782 working substance undergoes a change in temperature, pressure, volume, particle number,
 783 chemical association or disassociation, then that cycle or process has an entropy change
 784 intrinsic to its operation – heat is unavoidably generated. This of course includes Carnot cycle
 785 limited engines but it must include batteries, fuel cells and biochemical processes too. These
 786 latter categories are not thought of as heat engines but they must be: one has only to look at
 787 the change in standard entropies of the reactants and products and note that this change is
 788 part-and-parcel to their operation!

789
 790 We make the assertion that amongst heat engines, that there is a continuum from pure heat
 791 conduction, to Carnot limit engines, to fuel cells and biological systems to Maxwell Demon
 792 processes (fig. 28).



793
 794

795 **Figure 28 – The continuum of heat engines**

796
 797 The chart shows from the point of view of efficiency how particular types of engine fit into
 798 the continuum scheme. Logically to the left at zero efficiency, where any heat we might
 799 develop is wasted in heat conduction. Next comes the Carnot cycle limited engines we can
 800 deliver some useful work up to their efficiency limit.

801
 802 Next, we insist (for the argument given previously) must be the position of batteries, fuel
 803 cells and biological systems as heat engines. It is known that they exceed Carnot efficiency
 804 and indeed, E. T. Jaynes[21] in a contentious unpublished work took the Carnot reasoning
 805 applied to a muscle to an illogical conclusion, that living muscles must be operating at some
 806 6000K to achieve their work output! Correctly Jaynes points out that the degrees of freedom
 807 for the release of chemical energy are very curtailed, unlike the random motion of linear
 808 motion being cohered from a piston in a Carnot cycle, muscles fibres extend and contract in
 809 one very specific direction under the control of ATP. Try as one might to deny that fuel cells

810 and biological systems aren't heat engines, one cannot deny the change in entropy of the
811 reactants.

812

813 We think our diagram (fig. 28) makes it clear that one can utilise heat energy much more
814 subtly than a Carnot cycle. The continuum from the middle ground and especially biological
815 systems to Maxwell Demon type processes becomes apparent. Moving to the limit of the
816 middle sector of figure 28, Mae-Wang-Ho[22] has argued that some biochemical processes
817 (especially enzyme catalysis) utilise random thermal motion to achieve more than can be
818 explained by conventional thermodynamics – an input of heat energy from the environment
819 in addition to that from chemical sources is needed to explain the work, such as surmounting
820 the activation energy requirement. Thus in the right sector of figure 28, we include the
821 possibility where there is no energy input and the work is achieved wholly by the conversion
822 of environmental heat energy input – a Maxwell Demon.

823

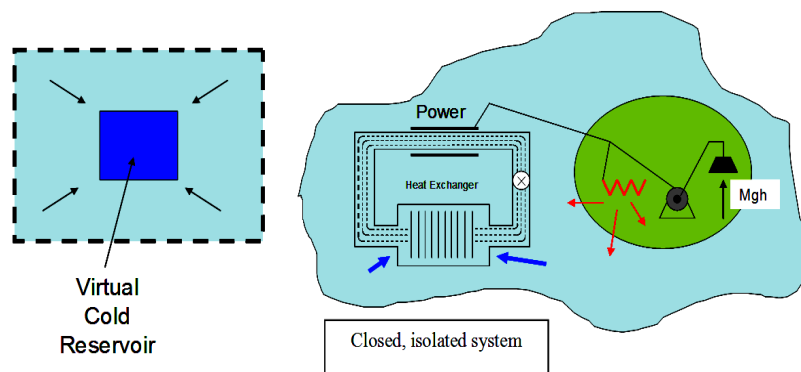
824

825 **6. Severing the link between Information Theory and** 826 **Physics?**

827

828 Boltzmann's identification of entropy as related to the microstates of a system, the Maxwell
829 Demon thought experiment and then the analyses of Szilard and then Brillouin was meant to
830 bring information into the fold of physics, even though information concepts of Turing and
831 Shannon[23] seemed abstract. Information was seen as a branch of thermodynamics, leading
832 to the celebrated maxim of Rolf Landauer, "Information is physical". However the concepts
833 and experiments discussed in this conference raise the prospect of de-facto reversible
834 computing by heat recovery; it doesn't matter if we try to make each logic step reversible
835 rather than use a conventional computer and recover the heat energy expended by it, it
836 amounts to the same thing. How then can the claim that information is branch of
837 thermodynamics be upheld?

838



839

840

841 **Figure 29 – A Thermodynamic Paradox – macroscopic work at constant entropy**

842

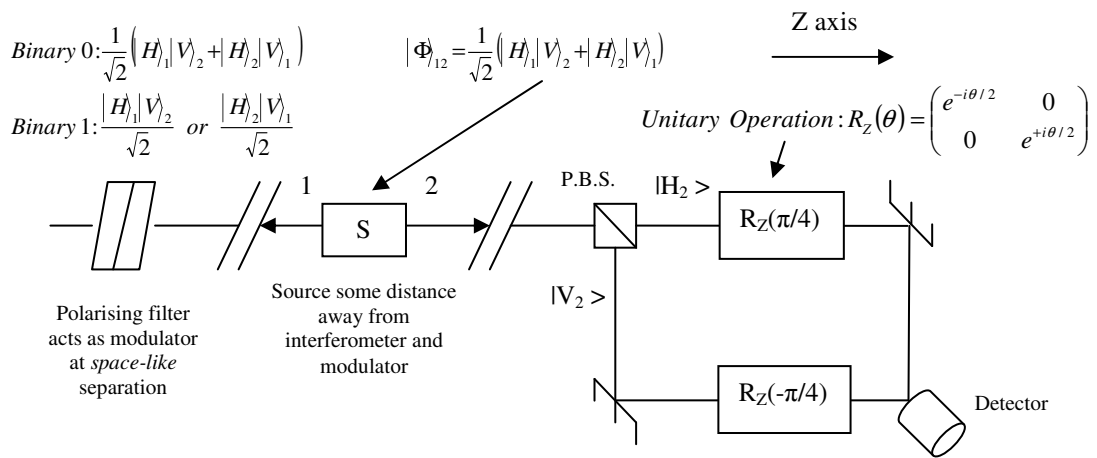
843 A further development is work by the author on the ultimate speed of information transit in
844 abeyance of Relativity. Utilising a classical protocol over a quantum channel[24, 25], the
845 author claims a disproof of the "No-communication" theorem[26]. The essence of this is to
846 send an entangled state between two parties ("Alice" and "Bob") so that the latter can discern
847 a pure (corresponding to the entangled and unmeasured state by the former) and the mixed
848 state (corresponding to the un-entangled and measured state by the former), thus

849 implementing a digital protocol (fig 30, this can also be achieved by single particle path
 850 entanglement[25] too, fig. 31). The speed of wavefunction collapse appears extremely
 851 fast[27], if not *instantaneous* for reason of the conservation of probability current. If the
 852 transfer of this “influence” cannot obey a wave equation in some manner,
 853

$$\frac{\partial^2 \psi}{\partial t^2} = \frac{1}{c^2} \frac{\partial^2 \psi}{\partial x^2}$$

854
 855
 856 how can the process claim to be *physical*? Physics is understood as the interplay of energy,
 857 matter, space and time.
 858

859 **Figure 30 – Transmitting classical data down a entangled two-particle**
 860 **quantum channel**



Measurement/Modulation at distant system and state of two photon system	State of distant system	State of local system	Local measurement by <u>interferometer</u> after modulation of distant system
875 No modulation: 'Binary 0' 876 $\frac{1}{\sqrt{2}} (H\rangle_1 V\rangle_2 + H\rangle_2 V\rangle_1)$	877 Entangled => Pure state 878 $\frac{1}{\sqrt{2}} (H\rangle_1 + V\rangle_1)$ 879 (Or at least some 880 superposition)	877 Entangled => Pure state 878 $\frac{1}{\sqrt{2}} (V\rangle_2 + H\rangle_2)$	877 Pure state results in 878 interference 879 (Or at least some interference 880 since source is not ideally 881 pure)
882 Modulation: 'Binary 1' 883 $\frac{ H\rangle_1 V\rangle_2}{\sqrt{2}}$ or $\frac{ H\rangle_2 V\rangle_1}{\sqrt{2}}$	882 Not entangled <=> 883 Mixed state $\frac{ H\rangle_1}{\sqrt{2}}$ or $\frac{ V\rangle_1}{\sqrt{2}}$	882 Not entangled <=> 883 Mixed state $\frac{ H\rangle_2}{\sqrt{2}}$ or $\frac{ V\rangle_2}{\sqrt{2}}$	882 Mixed state gives 883 no interference

884
 885 **Table 1 – The protocol for transmitting classical data down a**
 886 **quantum channel**

887
 888
 889
 890
 891
 892 Clearly to manifest, information takes on physical form as matter or photons but to use a
 893 computing engineering analogy, a Java virtual machine[28] (or any virtual machine) can run
 894 on any platform: processor or operating system, then information must take on a
 895 mathematical, meta-physical aspect too; it can somehow just exist abstractly. This deeply
 896 philosophical matter is related to the idea of whether mathematics is created or discovered (as
 897 one might perform an experiment and find a law of nature).

898
899
900
901
902
903
904
905
906
907
908
909
910
911
912
913

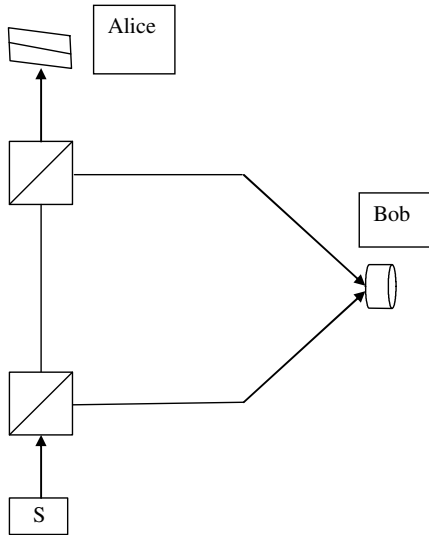


Figure 31 – Single photon path entanglement to send classical data over a quantum channel

The path lengths and cancellations are implied. The source, S, is a single photon transmitter incident upon two beam splitters.

“Alice” lets pass or absorbs the *wavefunction* such that “Bob’s” interference pattern either in the mixed state or cancels/reinforces respectively.

914
915
916
917
918
919
920
921
922

Some theoretical physicists would probably like to believe that all Creation is mathematics. A computer scientist can create a virtual universe on a computer by a combination of software (algorithms and equations) running on hardware governed by physical principles. In mathematical physics there is no dichotomy between software and hardware... nature’s laws need no computer to run, they seem to bootstrap and have a life of their own. Indeed, as already mentioned, real Maxwell Demons do just that in abeyance of our computing model that has the requirement that state information be kept. The self-computing ability of mathematical-physics laws is most puzzling.

7. Conclusion

923
924
925
926
927
928
929
930
931
932

This paper has laid out the theory and engineering required to generate sizeable quantities of heat from a single reservoir by a magneto-calorific-kinetic process. The status of the research is on-hold for further funding to pursue ferrofluid development. However it is clear by standard theory (thermodynamics, kinetic and electrodynamic), provisional experiments and computer simulations, that there would need to be a “ghost in the machine”, “a cosmic censor” or some “anti-demon” to suspend kinetic theory and prevent the process from occurring. Given the successes of Sheehan[1] and others, this seems unlikely.

933
934
935
936
937
938
939
940
941

The author clearly identified the type of mechanism and reason for the operation for this type of phase transition demon: at the kinetic level a molecular sorting was identified for 1st order[29] and 2nd order transitions; furthermore on T-S or work diagrams, an addition to the thermodynamic identity was noted which rendered it inexact around a cycle. This allowed a break from the traditional isothermal-adiabatic-isothermal-adiabatic of the Carnot cycle and the necessary rejection of heat to a lower reservoir; thus heat energy could be obtained from one reservoir in abeyance of the Kelvin-Planck/Clausius statements of the 2nd law. Purely theoretically, this simple proof is enough to call into question Carnot’s theorem.

942
943
944
945
946
947

The author then challenged the general ignorance that only Carnot cycle limit engines are heat engines. Logically, if the start and end states of a process or cycle experience an intrinsic change in entropy (not just something that can be engineered out or minimised, such as flow resistance), then it too is an heat engine. This definition brings batteries, fuel cells and even life into the fold. The suggestion that catalysis or even enzyme catalysis benefits from thermal motion, leads one to the belief that these are over-unity heat engines, delivering more

948 “bang for the buck” than the simple input of chemical energy would have us believe – bear
949 witness to the activation energy. Another consideration in biological systems, due to E. T.
950 Jaynes[21], is that biological systems may be severely limiting the degrees of freedom in
951 liberating chemical energy and achieving efficiencies way beyond the random energy input to
952 a Carnot cycle limited process. In fact, upon comparing muscle to a Carnot cycle, Jaynes
953 calculates that a muscle’s temperature would need to be in excess of 6000K! It is a natural
954 step in this continuum of heat engines: from Carnot to thermal agitation enhanced catalysis to
955 the over-unity Maxwell Demon, where the thermal bath energy input exceeds any energy
956 input (indeed, those auxiliaries are powered by the power generated).

957

958 Discussion

959

960 To conclude, the author then wondered if the link between thermodynamics and information
961 theory was warranted. De-facto reversible computing will be possible by the methods
962 presented in this conference. Where is then this “cost” of information? If the link to
963 thermodynamics was severed, the author highlighted another area of their work related to the
964 ultimate speed of transit of information. Entanglement correlation over space-like intervals is
965 well known. The author has a disproof of the “No communication theorem” and two schemes
966 for avoiding the randomness of quantum measurement, indeed to utilise it to an advantage,
967 such that classical data can be sent over space-like separations. What then is the link of
968 information to Relativity or physics in general?

969

970 This reasoning suggests something profound, mathematical and even metaphysical about
971 information. Rolf Landauer’s maxim “Information is physical” cannot be entirely true. An
972 aspect of information seems implementation independent, much as virtual machines (ie. Java)
973 are to hardware and operating systems. The author believes that mathematical physics has
974 some independent “life” – it needs no hardware to run; to quote a private correspondence
975 between the author and D. Sheehan, his words were “it just goes”. This is very pertinent to
976 the Demon problem – the Szilard/Brillouin/Landauer/Bennet view is that the decision making
977 machinery of the demon must reject information and this step involves the rejection of heat.
978 We are saying that the hardware-software dichotomy doesn’t exist for the Demon, the
979 equations describing the particle interactions of the sorting process “just go”.

980

981

982 The final status of the 2nd law is of course generally true, if there are energy dissipation
983 processes. Maxwell Demon processes form an exception to this, with the possibility of
984 regions of zero change or decreasing entropy. However there is a problem with saying that
985 the Arrow of Time is synonymous with the increase in entropy. A large region of space could
986 form an isolated environment with these heat-reuse engines. Life would go on, live, die,
987 evolve and there is much change, yet the global entropy change for this region would be zero.
988 We must search elsewhere for the Arrow of Time; given now our knowledge of chaotic
989 dynamics or even the quantum measurement process, the Arrow of Time is obviously Loss of
990 Information.

991

992

993

References

- 994
995
996
997 1. D.P. Sheehan, D.J.Mallin.e.a., *Experimental Test of a Thermodynamic Paradox*.
998 Found Phys, 2014. **44**.
- 999 2. D'Abramo, G., *Thermo-charged capacitors and the Second Law of Thermodynamics*.
1000 Phys. Lett. A, 2010. **374**: p. 1801-1805.
- 1001 3. Sheehan, D.P., *The Second Law of Thermodynamics:*
1002 *Foundations and Status*. Found Phys, 2007. **37**: p. 1653-1658.
- 1003 4. V. Čápek, D.P.Sheehan., *Challenges to the Second Law of Thermodynamics*. 2005:
1004 Springer.
- 1005 5. Jackson, J.D., *Classical Electrodynamics*. 2nd ed. 1975: Wiley.
- 1006 6. Landau, L., *A Course in Theoretical Physics: Classical Theory of Fields*. Vol. Vol. 2
1007 1982: Butterworth-Heinemann.
- 1008 7. Feynman, L., Sands, *The Feynman Lectures on Physics*. Addison-Wesley, Reading,
1009 Massachusetts. Vol. Vol.1, Vol. 2 1989. 14.7, 15.1-6, 35.4
- 1010 8. Bozorth, R.M., *Ferromagnetism*. IEEE Press 1978.
- 1011 9. Aharoni, A., *Introduction to the Theory of Ferromagnetism*. Oxford Science
1012 Publications 1996.
- 1013 10. Kittel C., K.H., *Thermal Physics*. W. H. Freeman and Company, San Francisco. Vol.
1014 2nd ed. 1980.
- 1015 11. Rosensweig, R.E., *Ferrohydrodynamics*. Cambridge University Press. 1998.
- 1016 12. Cornwall R. O., *Novel Thermodynamic Cycles involving Ferrofluids displaying*
1017 *Temporary Magnetic Remanence*. 2013(<http://vixra.org/abs/1311.0078>).
- 1018 13. Gschneidner, K.A., Jr.; Pecharsky, V. K., *Recent developments in magnetocaloric*
1019 *materials*. IOP Reports on Progress in Physics, 2005. **68**(6): p. 1479–1539.
- 1020 14. J. Romero Gómez, R.F.G., A. De Miguel Catoira, M. Romero Gómez,
1021 *Magnetocaloric effect: A review of the thermodynamic cycles in magnetic*
1022 *refrigeration*. Renewable and Sustainable Energy Reviews, 2013. **17**: p. 74-82.
- 1023 15. Landau, L., *A Course in Theoretical Physics: Statistical Physics*. Vol. Vol. 5. 1996:
1024 Butterworth Heinemann.
- 1025 16. Vallejo-Fernandez, O.G., Patel, *Mechanisms of hyperthermia in magnetic*
1026 *nanoparticles*. J. Phys. D: Appl. Phys., 2013. **46**.
- 1027 17. Fannin, P.C., *A Study of the Complex Susceptibility of Ferrofluids and Rotational*
1028 *Brownian Motion*. Journal of Magnetism and Magnetic Materials, 1987. **65**: p. 279-
1029 281

- 1030 18. Fannin, P.C., *On the Analysis of Complex Susceptibility Data of Ferrofluids*. Journal
1031 of Physics D: Applied Physics, 1988. **21**: p. 1035-1036
- 1032 19. Landau, L., *A Course in Theoretical Physics: Kinetics*. Vol. Vol. 10. 1981:
1033 Butterworth-Heinemann.
- 1034 20. Haile J. M., *Molecular Dynamics Simulation*. 1997: John Wiley and Sons.
- 1035 21. Jaynes, E.T., *The muscle as an engine*.
1036 1983(<http://bayes.wustl.edu/etj/articles/muscle.pdf>).
- 1037 22. Ho, M.-W., *The Rainbow and the Worm: The Physics of Organisms*. 2nd ed: World
1038 Scientific.
- 1039 23. Harvey L. S., A.F.R., *Maxwell's Demon: Entropy, Information and Computing*. Adam
1040 Hilger, Bristol 1991.
- 1041 24. Cornwall, R.O., *Secure Quantum Communication and Superluminal Signalling on the
1042 Bell Channel*. Infinite Energy, 2006. **69**(<http://vixra.org/abs/1311.0074>).
- 1043 25. Cornwall, R.O., *Superluminal Signalling by Path Entanglement*.
1044 2015(<http://vixra.org/abs/1410.0113>).
- 1045 26. Cornwall, R.O., *Disproof of the No-communication Theorem by Decoherence Theory*.
1046 2015(<http://vixra.org/abs/1506.0068>).
- 1047 27. Zbinden, H.G., N., et al, *Testing the speed of 'spooky action at a distance'*. Nature,
1048 2008. **454**.
- 1049 28. Sun-Microsystems/Oracle, *The Java™ Tutorials*.
1050 <http://docs.oracle.com/javase/tutorial/>.
- 1051 29. Cornwall, R.O., *How to build a Maxwell Demon from a 2nd order Phase Change
1052 System*. 2013(<http://vixra.org/abs/1311.0077>).
- 1053 30. Landau, L., *A Course in Theoretical Physics: Mechanics*. Vol. Vol. 1. 1982:
1054 Butterworth Heinemann.
- 1055 31. *The Ergodic Theorem*, in *Encyclopaedia Britannica Inc*.
- 1056 32. Jordan D. W., S.P., *Nonlinear Ordinary Differential Equations*. Clarendon Press
1057 Oxford. Vol. 2nd ed. . 1991.
- 1058 33. Kapitaniak, T., *Chaos for Engineers*. Springer 1998.
1059
1060
1061